



Utilisation of Winery Waste Biomass in Fluidised bed Gasification and Combustion

Philip van Eyk and Peter Ashman

South Australian Coal Research Laboratory
School of Chemical Engineering
The University of Adelaide, SA, Australia

Date: 10 May 2010

Prepared for:

Richard Muhlack
The Australian Wine Research Institute
Hartley Grove, Urrbrae (Adelaide) SA 5064

Executive Summary

Australian wineries produce waste biomass in the form of winery residues, including grape marc, stalks and stems. This biomass is being considered as a potential fuel for generation of electricity by using a fluidised bed boiler or gasifier. Fluidised bed conversion of solid fuels is considered to be a mature technology with many large scale installations existing worldwide. Despite the maturity of the technology, challenges still exist when utilising biomass and waste fuels due to their variable nature, high moisture content, high alkali (ie. Na and K) content, and interactions between the bed material and ash that may lead to fouling and agglomeration within the fluidised bed environment. Consequently, good prior knowledge of the fuel and its combustion behaviour is important for the successful design and operation of biomass-fired Fluidised bed boilers.

This report presents results of a series of experiments undertaken on fluidised bed gasification and combustion of grape marc and grape stalks. Gasification and combustion experiments were undertaken in a Circulating Fluidised Bed (CFB) apparatus. The tests conducted in this work were primarily to establish whether gasification and combustion of grape marc or grape stalks causes bed material agglomeration and/or defluidisation. A secondary objective was to establish typical gas compositions that results from gasification of grape marc and grape stalks.

For the grape marc tests, smooth continuous operation was maintained for up to 200 minutes in all cases. There was a relatively steady temperature and the pressure drop over the bed rose only slightly over the period of test in each case due to the build up of ash and unburnt char in the bed. However, on close examination of the bed material collected after the CFB had cooled down, agglomerates of bed particles were discovered. Scanning Electron Microscopy (SEM) and X-Ray Diffraction were used to analyse the chemical, morphological and mineralogical nature of the agglomerates. Both gasification and combustion tests gave similar ash analyses using SEM, implying similar mechanisms for agglomerate formation. A possible mechanism for agglomerate formation was proposed where potassium carbonate (K_2CO_3) formed in the char reacts with silica from the bed material leading to the formation of molten potassium silicates.

For the grape stalk tests, serious problems were encountered during the start up period for gasification in most cases. There were large inconsistencies in the temperature in the bed, mostly brought about by problems in feeding the fibrous stalk particles to the CFB. SEM analysis of the bed material highlighted a possible mechanism for agglomerate formation during both combustion and gasification tests: potassium carbonate (K_2CO_3) and sodium chloride (NaCl) formed in the char reacts with silica from the bed material leading to the formation of molten potassium silicates.

During the gasification tests, useful information into gas compositions were gathered. Higher bed temperatures led to better the CO and H₂ concentrations, as well as the better conversion of carbon in the original biomass. The lack of steam in the system caused by the dry fuel used led to lower concentrations of H₂. Hence, the addition of wet fuel into the gasifier will increase the reactions with steam, thereby forming more H₂.

Further research to develop and verify mitigation strategies for agglomerate formation is required in order to utilize winery biomass for gasification or combustion at a large scale.

Table of Contents

1	INTRODUCTION	5
2	EXPERIMENTAL WORK	6
2.1	FUEL SAMPLING AND ANALYSIS	6
2.2	EXPERIMENTAL APPARATUS FOR GASIFICATION AND COMBUSTION TESTING	8
3	RESULTS AND DISCUSSION.....	10
3.1	EXPERIMENT SUMMARY.....	10
3.2	STAGE I RESULTS: GASIFICATION OF MARC.....	11
3.2.1	<i>Stage I observations</i>	11
3.2.2	<i>SEM Analysis</i>	11
3.2.3	<i>XRD Analysis</i>	16
3.2.4	<i>Mechanism of Agglomeration</i>	17
3.2	STAGE II RESULTS: GAS COMPOSITIONS	18
3.3.1	<i>Experimental Observations</i>	18
3.3.2	<i>Gas Compositions and Carbon conversions</i>	18
3.4	STAGE III RESULTS	20
3.4.1	<i>Stage III observations</i>	20
3.4.2	<i>SEM Analysis</i>	20
3.4.3	<i>Mechanism of Agglomeration</i>	25
3.5	STAGE IV RESULTS.....	26
3.5.1	<i>Stage IV observations</i>	26
3.5.2	<i>SEM Analysis</i>	26
3.5.3	<i>Mechanism of Agglomeration</i>	30
4	CONCLUSIONS AND RECCOMENDATIONS	31
4.1	CONCLUSIONS FROM STAGE I.....	31
4.2	CONCLUSIONS FROM STAGE II.....	31
4.3	CONCLUSIONS FROM STAGE III	31
4.3	CONCLUSIONS FROM STAGE IV	32
4.5	RECOMMENDATIONS	32
6	REFERENCES	33
	APPENDIX A: TGA RESULTS FOR GRAPE MARC	34

List of Figures

FIGURE 1 – SCHEMATIC DIAGRAM OF THE CIRCULATING FLUIDISED BED APPARATUS	9
FIGURE 2 – SEM MICROGRAPH OF AN AGGLOMERATE FROM TEST G02	12
FIGURE 3 – SEM SPECIFIC ANALYSES ON A CARBON AND OXYGEN FREE BASIS OF FIG 2	12
FIGURE 4 – SEM MICROGRAPH OF THE CROSS SECTION OF AN AGGLOMERATE FROM TEST G02	13
FIGURE 5 – SEM SPECIFIC ANALYSES ON A CARBON AND OXYGEN FREE BASIS OF FIG 4	13
FIGURE 6 – SEM MICROGRAPH OF CHAR PARTICLE #1 FROM TEST G02	14
FIGURE 7 – SEM MICROGRAPH OF CHAR PARTICLE #2 FROM TEST G02	14
FIGURE 8 – SEM SPECIFIC ANALYSES ON A CARBON AND OXYGEN FREE BASIS OF FIG 6 AND 7	15
FIGURE 9 – SEM MICROGRAPH OF FUSED AGGLOMERATE FROM TEST G02	15
FIGURE 10 – SEM SPECIFIC ANALYSES ON A CARBON AND OXYGEN FREE BASIS OF FIG 9	16
FIGURE 11 – BED TEMPERATURE EFFECT ON GAS COMPOSITION	19
FIGURE 12 – CARBON CONVERSION VERSUS BED TEMPERATURE	19
FIGURE 13 – SEM MICROGRAPH OF FUSED AGGLOMERATE FROM TEST G12	21
FIGURE 14 – SEM SPECIFIC ANALYSES ON A CARBON AND OXYGEN FREE BASIS OF FIG 13	21
FIGURE 15 – SEM MICROGRAPH OF FUSED AGGLOMERATE FROM TEST G12	22
FIGURE 16 – SEM SPECIFIC ANALYSES ON A CARBON AND OXYGEN FREE BASIS OF FIG 15	22
FIGURE 17 – SEM MICROGRAPH OF THE CROSS SECTION OF AN AGGLOMERATE FROM TEST G12	23
FIGURE 18 – SEM SPECIFIC ANALYSES ON A CARBON AND OXYGEN FREE BASIS OF FIG 17	23
FIGURE 19 – SEM MICROGRAPH OF CHAR PARTICLE FROM TEST G13	24
FIGURE 20 – SEM SPECIFIC ANALYSES ON A CARBON AND OXYGEN FREE BASIS OF FIG 19	24
FIGURE 21 – SEM MICROGRAPH OF A FUSED AGGLOMERATE FROM TEST C01	27
FIGURE 22 – SEM SPECIFIC ANALYSES ON A CARBON AND OXYGEN FREE BASIS OF FIG 17	27
FIGURE 23 – SEM MICROGRAPH OF THE CROSS SECTION OF AN AGGLOMERATE FROM TEST C01	28
FIGURE 24 – SEM SPECIFIC ANALYSES ON A CARBON AND OXYGEN FREE BASIS OF FIG 23	28
FIGURE 25 – SEM MICROGRAPH OF AGGLOMERATE FROM TEST C02	29
FIGURE 26 – SEM SPECIFIC ANALYSES ON A CARBON AND OXYGEN FREE BASIS OF FIG 25	29
FIGURE 27 – SEM MICROGRAPH OF THE CROSS SECTION OF AN AGGLOMERATE FROM TEST C02	30
FIGURE 28 – SEM SPECIFIC ANALYSES ON A CARBON AND OXYGEN FREE BASIS OF FIG 27	30
FIGURE A1 – TGA RESULTS FOR GRAPE MARC IN N ₂ AT 30°C/MIN	35
FIGURE A2 – TGA RESULTS FOR GRAPE MARC IN N ₂ AT 5°C/MIN	36
FIGURE A3 – TGA RESULTS FOR GRAPE STALKS IN N ₂ AT 30°C/MIN	37
FIGURE A4 – TGA RESULTS FOR GRAPE STALKS IN N ₂ AT 5°C/MIN	38
FIGURE A5 – TGA RESULTS FOR GRAPE MARC IN AIR AT 30°C/MIN	39
FIGURE A6 – TGA RESULTS FOR GRAPE MARC IN AIR AT 5°C/MIN	40
FIGURE A7 – TGA RESULTS FOR GRAPE STALKS IN AIR AT 30°C/MIN	41
FIGURE A8 – TGA RESULTS FOR GRAPE STALKS IN AIR AT 5°C/MIN	42

List of Tables

TABLE I: ANALYSIS RESULTS FOR MOISTURE CONTENT, ASH YIELD, VOLATILES AND FIXED CARBON	7
TABLE II: ANALYSIS RESULTS FOR C, H, N, S, NA, K AND CL (% DRY BASIS)	7
TABLE III: ANALYSIS RESULTS FOR ASH COMPOSITION (% IN ASH)	7
TABLE IV: ANALYSIS RESULTS FOR GRASS DRY, GROSS WET, AND NET WET CALORIFIC VALUES	8
TABLE V: SUMMARY OF EXPERIMENTS PERFORMED	10
TABLE VI: MINERALOGICAL DETERMINATION FOR VARIOUS TESTS USING XRD	16
TABLE VII: COMPARISON BETWEEN SEM SPECIFIC ANALYSES ON A CARBON AND OXYGEN FREE BASIS FOR MARC AND STALKS GASIFICATION AGGLOMERATES	22
TABLE VIII: COMPARISON BETWEEN SEM SPECIFIC ANALYSES ON A CARBON AND OXYGEN FREE BASIS FOR MARC AND STALKS GASIFICATION	25

1 Introduction

Grape marc and stalks are solid waste products left over from the winemaking process and accounts for approximately 10-20% w/w of the annual crush each vintage. Marc consists of skins, seeds, juice/wine and some stalks. In 2009, over 170,000 tonnes of marc was estimated to have been generated throughout Australia [1]. Appropriate sustainable treatment and disposal of this waste material is an ongoing issue for the wine industry; if the marc is not treated effectively it can lead to a number of environmental hazards on disposal ranging from surface and groundwater pollution to foul odours.

Furthermore, the world is currently facing an ever-increasing energy demand, which together with a largely fossil fuel-based economy has resulted in increasing global CO₂ emissions and associated risks of harmful climate change. The Australian wine industry has recognised that it is particularly vulnerable to these risks [2], which come at a time of unprecedented energy and transport fuel costs as well as increasing competition from global wine markets and consumer awareness of environmental issues such as water use and carbon footprint.

Australian wineries currently rely upon grid-supplied electricity of which a significant proportion is generated by coal-fired power stations that are a major source of greenhouse gas emissions. However, an opportunity may exist for the wine industry to develop customized technology to produce its own renewable electricity from existing winery biomass waste streams such as grape marc and grape stalks.

Various forms of biomass are already used in other sectors as a CO₂-neutral energy source, despite their generally lower energy density [3]. Grape marc and stalks have been identified as a potential CO₂-neutral fuel for the generation of electricity by means of fluidised bed combustion or fluidised bed gasification coupled with a gas turbine or gas engine. Such an approach would further strengthen the sustainability of the Australian wine industry, which directly employs over 30,000 people [4] and is Australia's third largest agricultural export earner (2008 export sales in excess of A\$2.5 billion) [5].

Fluidised-bed conversion of solid fuels is a well-established and widely used technology and is ideally suited to biomass electricity applications. However despite its broad application, operational problems can occur. One of the most significant problems is the occurrence of agglomeration at high temperature, whereby bed particles adhere to each other to form larger entities (agglomerates) [6]. Usually, the conversion of the solid fuel is carried out with silica sand and ash as bed material. The formation of liquid-phases (melt) in the fluidised bed has been shown to be responsible for sintering, bed agglomeration, and bed defluidisation. Melts of the form of salts [7, 8], and silicates [9-11] have been reported. The dominant mechanisms for agglomeration of beds during gasification of biomass fuels have been shown to be: (a) Formation of low melting point calcium silicates for typical wood fuels, (b) direct attack by potassium compounds on the bed by forming low melting point potassium silicates for high alkali-containing biomass fuels, or (c) formation of potassium silicate particles/droplets within the fuel and consequent agglomeration for fuels containing both potassium and reactive silicon but to a lesser extent than other ash-forming elements [12].

The primary aim of this work was to investigate the potential occurrence and nature of any ash related problems from the fluidised bed gasification and combustion of grape marc and stalks. The secondary aim was to establish gas compositions resulting from fluidised bed gasification of winery waste biomasses.

2 Experimental Work

2.1 Fuel sampling and analysis

The biomass used in this work was grape marc and stalks collected in April 2009 from the Riverland region of South Australia. Tarac Technologies (Tarac) collects marc from wineries in the main wine producing states of South Australia, Victoria and New South Wales. Tarac process grape marc for the recovery of grape alcohol and tartaric acid. The bulk of the experiments were performed with the Post-Tarac red marc (processed by Tarac before collection), but Pre-Tarac red marc and the white marc were analysed to observe any obvious differences in the fuels. Composite samples of grape marc and stalks, collected over the period of 2007-2008 and mixed, was also analysed to determine any annual variations in the fuel or changes resulting from long term storage.

Analysis of each of the samples was performed by HRL Technology Pty Ltd. These analyses are shown in Tables I-IV.

Table I shows the analysis results for moisture content, ash yield, volatiles and fixed carbon. The moisture content of these samples was low due to pre-drying in an oven before the analysis. The original moisture content of the grape marc and stalk samples were assessed by weighing a given batch before and after placing in an oven overnight at 105°C. In this way it was determined that the raw grape marc and the raw stalks had moisture contents of ~65% and ~25% respectively. The proportions of volatile matter (VM) and fixed carbon (FC) were 67.2±1.9% and 25.7±1.5%. The biomass samples contain considerably more volatile matter and less fixed carbon in comparison to Victorian brown coals from the Gippsland region (VM~50.7% and FC~47.6) [13].

Table II shows the chemical composition of the biomass samples. For comparison, Victorian brown coals from the Gippsland region contain approximately 67.5% C, 4.9% H, 0.53% N and 0.98% S [13]. The potassium level of all the samples was extremely high (average of 1.8%). The stalks also contained significant sodium and chlorine contents. Potassium, sodium and chlorine are important because they cause fouling and agglomeration problems in gasifiers and combustors.

Table III shows the ash analysis of the biomass samples. It is clear that for all samples there are substantial quantities of K₂O, CaO and P₂O₅ in the ash. The Na₂O quantity in the stalks ash was up to an order of magnitude higher than the marc.

Table IV shows calorific values of the samples. The Gross Dry Calorific Value for the grape marc were on average 22.3 MJ/kg. This value is comparable to Victorian coals from the Gippsland region, which have Gross Dry calorific values of 26.4 MJ/kg on average [13].

Table I: Analysis results for Moisture content, Ash Yield, Volatiles and Fixed Carbon

Sample Description	Moisture (% as received)	Ash Yield (%dry basis)	Volatile Matter (%dry basis)	Fixed Carbon (%dry basis)
1 Pre-Tarac Red Marc	7.0	5.1	69.0	25.9
2 White Marc	5.4	6.5	67.7	25.8
3 Post-Tarac Red Marc	2.1	6.8	67.9	25.3
4 Composite 07-08 Marc	2.4	8.2	63.6	28.2
5 09 Grape Stalks	5.3	8.2	66.6	25.2
6 Composite 07-08 Stalks	2.4	7.8	68.5	23.7

Table II: Analysis results for C, H, N, S, Na, K and Cl (% dry basis)

Sample Description	C	H	N	S	Na	K	Cl
1 Pre-Tarac Red Marc	53.7	6.2	1.76	0.11	0.01	1.48	<0.01
2 White Marc	54.1	6.1	2.59	0.16	0.03	1.78	<0.01
3 Post-Tarac Red Marc	54.8	6.3	2.43	0.14	0.02	2.00	0.01
4 Composite 07-08 Marc	53.9	5.7	2.39	0.16	0.02	2.08	<0.01
5 09 Grape Stalks	49.2	5.3	1.15	0.24	0.31	1.68	0.38
6 Composite 07-08 Stalks	47.8	5.4	1.22	0.13	0.23	1.91	0.32

Table III: Analysis results for ash composition (% in ash)

Sample Description	LOI	SiO2	Al2O3	Fe2O3	TiO2	K2O	MgO	Na2O	CaO	SO3	P2O5	PbO	ZnO	Total
1 09 Pre-Tarac Red Marc	9.0	5.0	1.0	1.0	0.06	33.5	3.9	0.44	17.8	3.1	10.8	<0.01	0.04	85.7
2 09 White Marc	8.6	7.0	0.8	0.6	0.05	31.6	4.4	0.87	18.9	3.3	10.0	<0.01	0.03	86.2
3 09 Post-Tarac Red Marc	10.5	4.7	0.9	0.6	0.05	34.6	3.4	0.38	15.3	2.6	10.2	0.01	0.02	83.2
4 Composite 07-08 Marc	8.6	12.5	1.4	0.8	0.07	29.9	3.5	0.47	19.0	3.3	8.3	<0.01	0.04	87.9
5 09 Grape Stalks	3.6	7.8	2.2	0.5	0.09	22.6	9.5	5.38	25.5	7.8	4.1	<0.01	0.02	89.1
6 Composite 07-08 Stalks	3.6	4.6	1.0	0.5	0.06	30.3	7.3	4.38	19.3	2.5	5.5	<0.01	0.04	79.0

Table IV: Analysis results for Grass dry, gross wet, and net wet calorific values

Sample Description	Gross Dry Calorific Value	Gross Wet Calorific Value	Net Wet Calorific value
	(MJ/kg)	(MJ/kg)	(MJ/kg)
1 Pre-Tarac Red Marc	22.2	20.7	19.4
2 White Marc	22.3	20.8	19.5
3 Post-Tarac Red Marc	22.9	21.9	20.6
4 Composite 07-08 Marc	21.9	20.7	19.4
5 09 Grape Stalks	19.1	17.5	16.4
6 Composite 07-08 Stalks	13.1	12.2	11.0

2.2 Experimental Apparatus for gasification and combustion testing

Gasification and combustion experiments were undertaken in a Circulating Fluidised Bed (CFB) apparatus, shown schematically in Figure 1. The CFB consists of a 76mm (I.D.) stainless steel cylindrical furnace, with a conical section at its base. The furnace can be heated with four electrically heated elements located alongside the furnace tube. The furnace is fitted with a biomass hopper and feeder, primary and secondary cyclone separators for ash separation from the exhaust gases, and an unburnt char recirculation system. The reactor is also fitted with thermocouples and differential pressure probes along its height, which are interfaced to a PC to track changes in temperature and pressure in a run. There is a glass-covered viewing port at the top of the combustor.

A multi-hole distributor is connected to the bottom of the conical section and provides a spout of fluidising hot air, which is heated in an electric honeycomb-design air pre-heater to a temperature of 500°C. The distributor is designed to allow it to be removed at the end of an experiment in order to collect the spent bed material from the combustor in the bottom ash can.

The gasification or combustion of biomass takes place in the lower part of the furnace in a fluidised bed consisting of inert bed material (sand), partially gasified/combusted biomass char, and ash. Exhaust gases pass first through a primary cyclone separator and then through a secondary cyclone separator. Solid material collected in the primary cyclone, consisting of particles larger than approximately 0.2mm, is returned to the fluidised bed via a recirculation pipe. The smaller particles are separated in the secondary cyclone and collected in the Fly Ash can.

At the start of an experiment, 200g of sand (sieved to the range 0.25-0.5mm) was loaded into the gasifier and fluidised with 60L/min of air. The air pre-heater and external heating elements were used to heat the sand bed to approximately 700°C prior to the introduction of biomass. Once this temperature was reached, biomass feeding commenced, at which point combustion of the biomass together with the external heating elements supplied the extra heat needed to raise the bed to the required temperature for each experiment run (from 810°C to 910°C). The combustion air was then reduced to approximately 35 L/min in order to bring the fluidisation velocity to

approximately 1m/s and maintain an air-to-fuel ratio (A/F) necessary to achieve gasification or combustion.

The marc and stalk samples (as received) had moisture contents of ~65% and ~25% respectively, and so were air dried in an oven overnight prior to size reduction and fuel testing. The dried biomass was crushed and sieved in the range of 1.0-3.35mm prior to each experiment. Preliminary experiments revealed that optimal gasification performance at an airflow of 35 L/min was achieved with a biomass feed rate of ~1.5 kg/h, whereas optimal combustion performance was achieved with a biomass feed rate of ~0.5 kg/h. These flowrates were employed in all subsequent experiment runs.

To determine the gas compositions obtained from gasification of grape marc, samples were taken via a small valve and tube located in the freeboard of the gasifier using a Teflon sample bag. The contents of each sample bag was then analysed immediately using an Agilent 3000 micro Gas Chromatograph (micro GC).

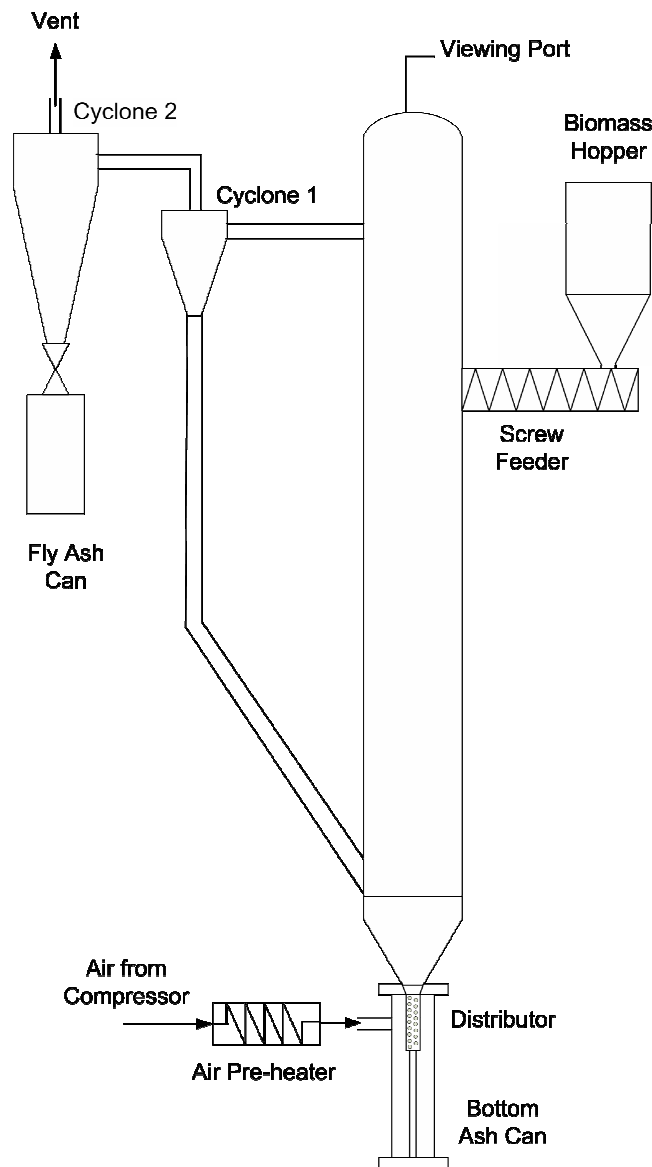


Figure 1 – Schematic diagram of the Circulating Fluidised Bed apparatus

3 RESULTS AND DISCUSSION

3.1 Experiment Summary

The gasification tests performed to determine agglomeration/defluidisation behaviour of grape marc and stalks in both Fluidised bed gasification and combustion. A summary of these experiments are shown in Table V.

Table V: Summary of experiments performed

Test ID	Test type	Test Objective	Bed temp.	Run Time	Comments
			°C	Minutes	
STAGE I	Gasification of Marc				
G01	Gasification of Pre-Tarac Red Marc	Agglomeration/Defluidisation	860	200	Agglomerates found
G02	Gasification of Post-Tarac Red Marc	Agglomeration/Defluidisation	860	200	Agglomerates found
G03	Gasification of White Marc	Agglomeration/Defluidisation	860	200	Agglomerates found
G04	Gasification of Post-Tarac Red Marc (Char Bed)	Ash Chemistry	860	60	-
STAGE II	Gas Compositions				
G05	Gasification of Marc	Gas Composition	810	30	-
G06	Gasification of Marc	Gas Composition	830	30	-
G07	Gasification of Marc	Gas Composition	850	30	-
G08	Gasification of Marc	Gas Composition	870	30	-
G09	Gasification of Marc	Gas Composition	890	30	-
G10	Gasification of Marc	Gas Composition	910	30	-
STAGE III	Gasification of Stalks				
G11	Gasification of Stalks	Agglomeration/Defluidisation	860	20	Defluidisation and Agglomeration
G12	Gasification of Stalks	Agglomeration/Defluidisation	860	20	Defluidisation and Agglomeration
G13	Gasification of Stalks (Char bed)	Agglomeration/Defluidisation	860	20	Defluidisation and Agglomeration
G14	Gasification of Stalks/Marc	Agglomeration/Defluidisation	860	30	Defluidisation and Agglomeration
G15	Gasification of Stalks/Marc	Agglomeration/Defluidisation	860	100	Agglomerates found
STAGE IV	Combustion Tests				
C01	Combustion of Marc	Agglomeration/Defluidisation	860	200	Agglomerates found
C02	Combustion of Stalks/Marc	Agglomeration/Defluidisation	860	60	Agglomerates found

3.2 Stage I Results: Gasification of Marc

3.2.1 Stage I observations

The tests in this series were conducted to establish whether gasification of grape marc causes bed material agglomeration and/or defluidisation. Stage I tests were Tests G01-G04 presented in Table II.

For Tests G01-03, smooth continuous operation was maintained for 200 minutes. Test G04 was only run for 60 minutes to obtain a sample of gasified grape marc char for mineralogical analysis. There was a relatively steady temperature in the bed of 860°C. The pressure drop over the bed rose slightly over the period of test in each case due to the build up of ash and unburnt char in the bed. From these observations, it was thought that problem-free continuous operation of a gasifier running on grape marc was a strong possibility. However, on close examination of the bed material collected after the CFB had cooled down, agglomerates of bed particles were discovered.

Samples were hence analysed for ash chemistry to determine the mechanism of agglomerate formation, and whether these agglomerates are likely to cause problems for continuous operation in a larger scale fluidised bed gasifier. Samples were analysed using Scanning Electron Microscopy (SEM) and X-Ray Diffraction (XRD). SEM was used to examine formation and morphology of bed material agglomerates, morphology of ash coating on the bed sand material and to analyse the chemical composition of these materials. XRD provides useful information about the minerals present in an examined material, as well as an order of magnitude determination of the proportion of individual minerals in a sample.

3.2.2 SEM Analysis

Samples of bed material and char taken from test G02 – Gasification of Post Tarac Red Marc were analysed using SEM. Particular efforts were made to find if the examined bed materials contained any agglomerates not visible to the naked eye, and the compositions of the joints between particles. Figure 2 shows an SEM micrograph of an agglomerate from Test G02. An analysis of the chemical composition of the frames 1 and 2 and spot 3 are given in Figure 3. All analyses of chemical compositions are expressed on a carbon and oxygen free basis.

Figure 3 shows that the ash coating on the bed material is consistently high in potassium, reflecting the high potassium content present in the original grape marc ash (see Table II). There are also significant quantities of calcium, phosphorus and magnesium present in the coating. Conversely, the silicon content is low, indicating the the silica sand particles are fully coated in an ash layer, and any silica in the analysis is likely originated from the grape marc ash. Although Figure 2 clearly shows a large agglomerate, it is unclear how the particles are joined due to a lack of obvious fused “glassy” coatings.

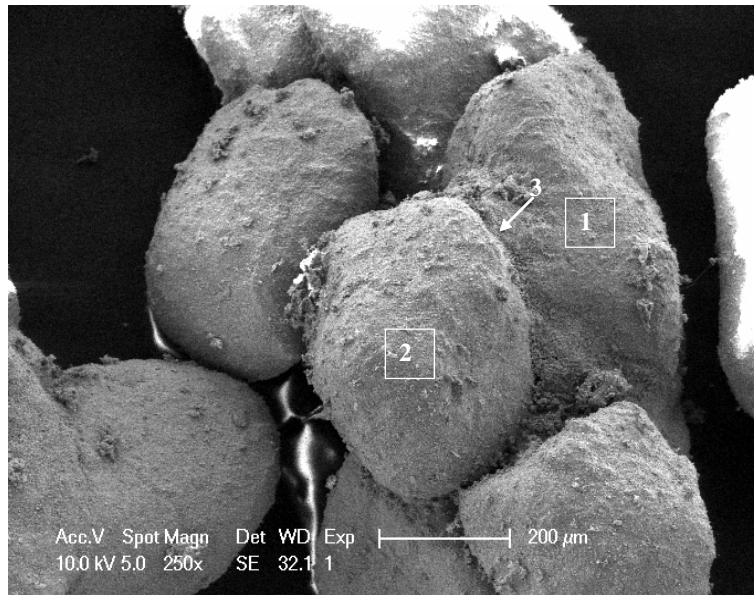


Figure 2 – SEM micrograph of an agglomerate from Test G02

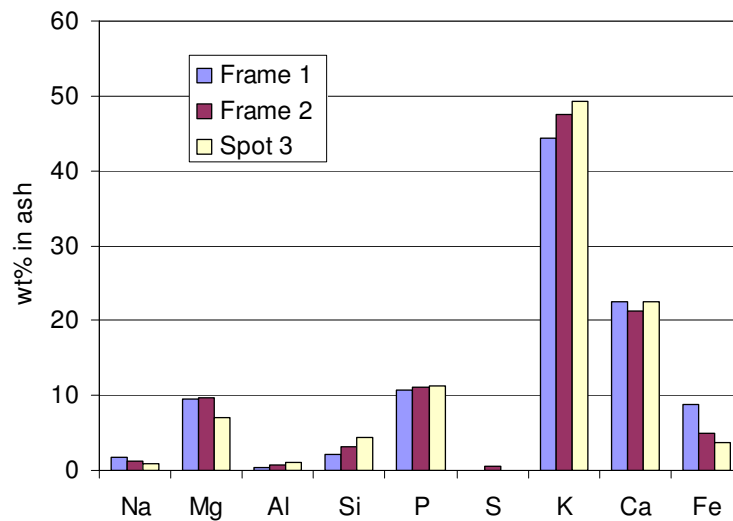


Figure 3 – SEM specific analyses on a carbon and oxygen free basis of Fig 2

Figure 4 shows an SEM micrograph of the cross section of an agglomerate from Test G02. An analysis of the chemical composition of the spots 1 and 2 are given in Figure 5. All analyses of chemical compositions are expressed on a carbon and oxygen free basis.

Figure 4 and 5 show that the sticky layer on all of the bed material is consistently high in potassium, reflecting the high potassium content present in the original grape marc ash (see Table II). The silicon content is also high in the sticky layer indicating that the potassium has diffused into the sand particles.

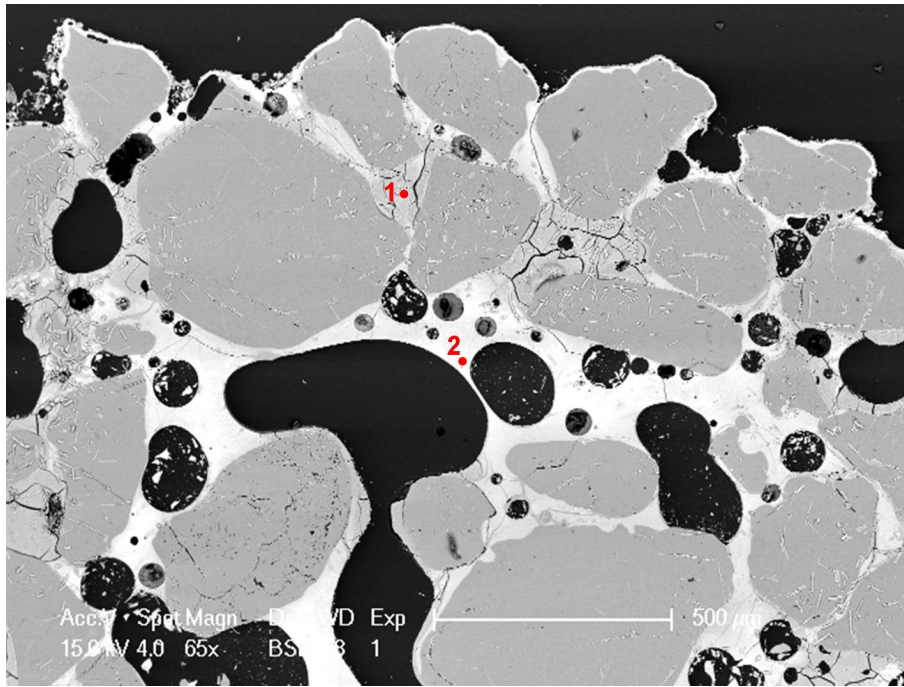


Figure 4 – SEM micrograph of the cross section of an agglomerate from Test G02

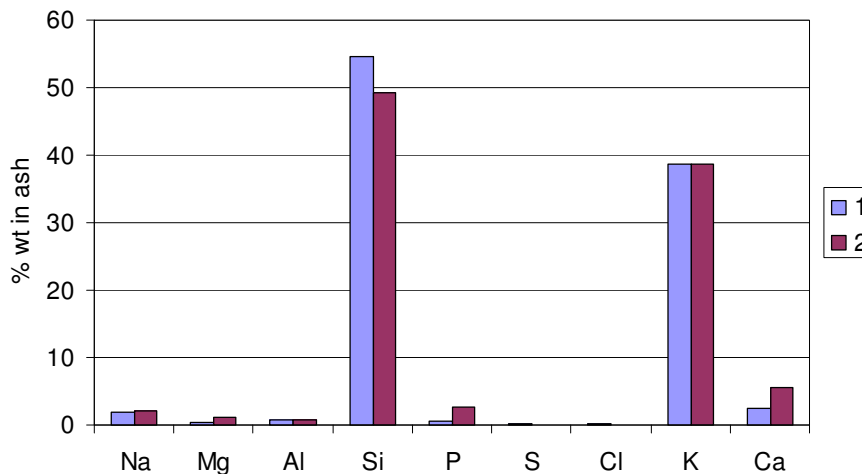


Figure 5 – SEM specific analyses on a carbon and oxygen free basis of Fig 4

The next SEM analysis was on the unburnt char particles within the bed. Figure 6 and 7 show SEM micrographs of two unburnt char found within the bed. Figure 8 shows the analysis of the chemical composition for Figure 6 and 7. It is seen that the potassium content is 60-70% on the surface of the char particles. This fact will be utilised in section 3.2.4 to help explain the mechanism for agglomeration during fluidised bed gasification of grape marc.

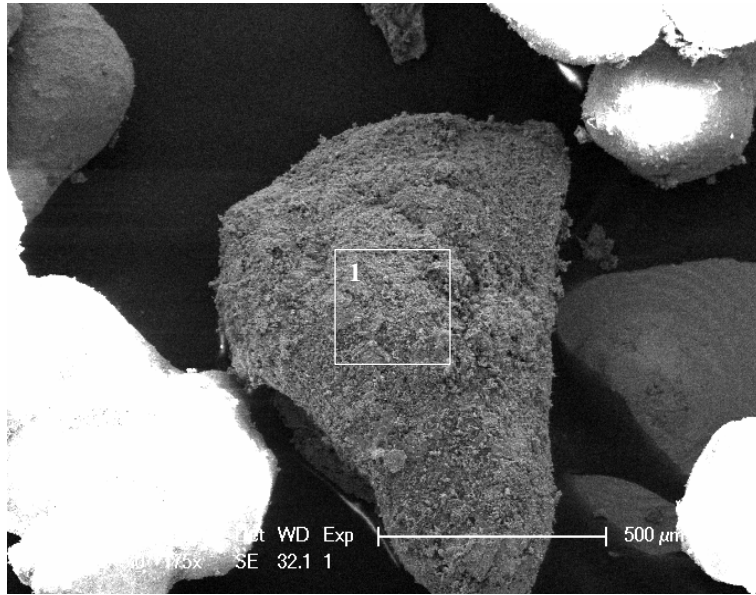


Figure 6 – SEM micrograph of char particle #1 from Test G02

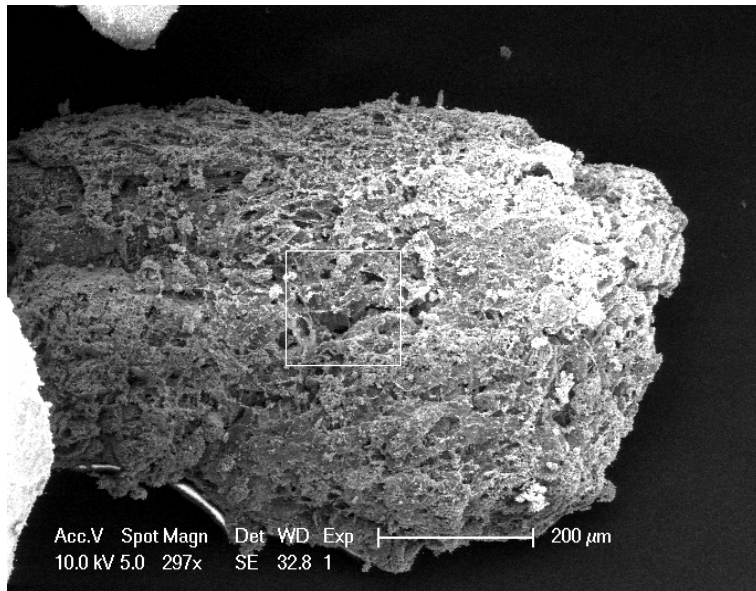


Figure 7 – SEM micrograph of char particle #2 from Test G02

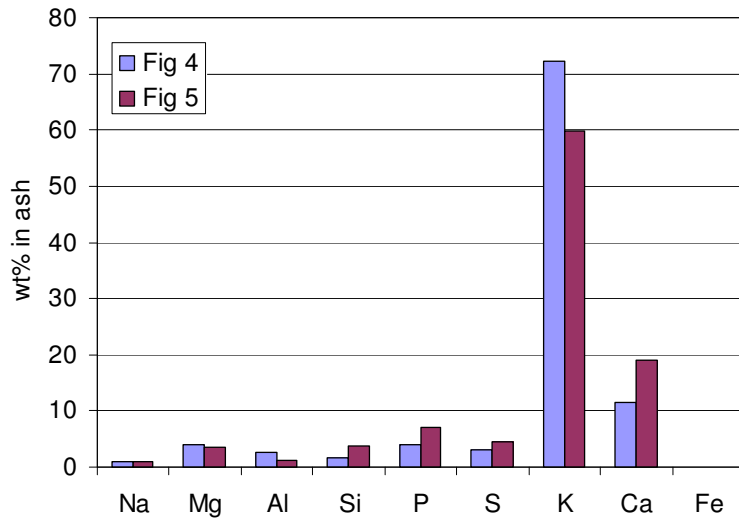


Figure 8 – SEM specific analyses on a carbon and oxygen free basis of Fig 6 and 7

The final SEM analysis was performed on a fused agglomerate. Figure 9 shows a SEM micrograph of a clearly fused agglomerate found within the bed, and Figure 10 shows the analysis of the chemical composition for Frames 1 and 2 in Figure 9. It can be seen in Figure 9 in the region of frame 1 that the chemicals present are fused/glossy in nature. The nature of this region is a non-crystalline substance. Referring to Figure 10 it is possible to infer that this substance is a potassium silicate glass, which would occur in liquid form at the temperatures of gasification. In contrast, Frame 2 appears to have a similar chemical nature as the ash layer on the agglomerate in Figure 2.

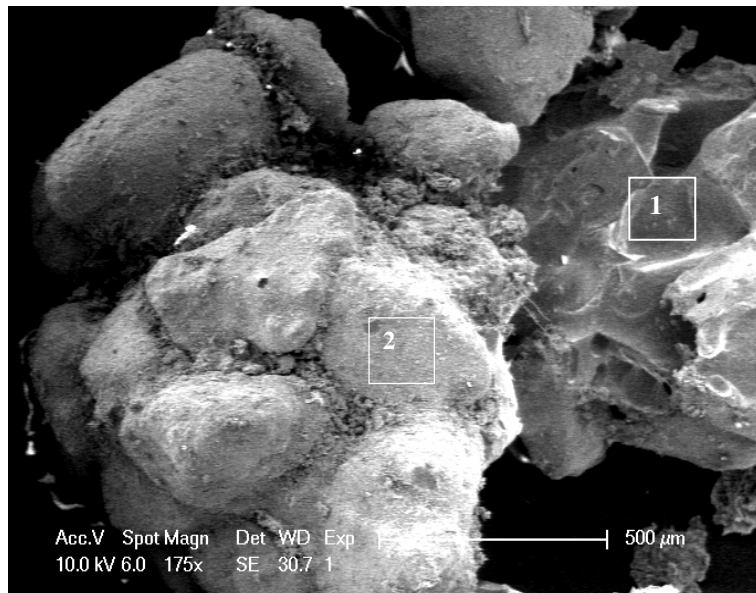


Figure 9 – SEM micrograph of fused agglomerate from Test G02

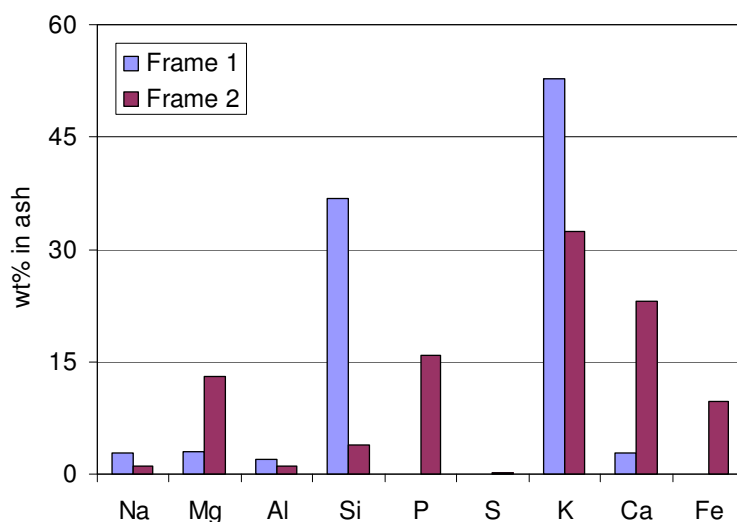


Figure 10 – SEM specific analyses on a carbon and oxygen free basis of Fig 9

The combination of the findings in Figures 2 – 10 suggests that the mechanism for agglomerate formation may involve the reaction of potassium from the char, with silicon from the bed material leading to the formation of molten potassium silicates. The form of potassium in the char has been determined by XRD, as discussed next.

3.2.3 XRD Analysis

In order to gain a better understanding of the minerals formed during gasification of grape marc, mineralogical analysis using X-ray diffraction (XRD) analysis was performed on some examples of bed material and fly ash. Analysis was performed by CSIRO Land and Water. The samples tested were Bed material and Fly ash from Test G02 – Post Tarac Red Marc Gasification, and Bed Material from Test G04 – Post Tarac Red Marc Gasification in a Char Bed. The summary of the results are presented in Table VI.

Table VI: Mineralogical determination for various tests using XRD

Sample Description	Minerals Present
1 Bed Material – Test G02	Quartz (D), K-Ca phosphate (KCaPO ₄)(T)
2 Fly Ash – Test G02	Kalclinite (CD), K-Ca phosphate (CD), periclase (M), calcite (M), anhydrite (T), dolomite (T)
3 Bed Material – Test G04	Kalclinite (D), K-Ca phosphate (M), calcite (T), anhydrite (T), dolomite (T)

D = dominant; CD = co-dominant; M = minor; T = trace

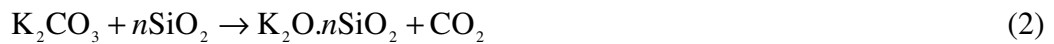
A major mineral phase determined by XRD in the Fly Ash of Test G02 and the Bed of Test G04 was Kalclinite, potassium bicarbonate (KHCO₃). Kalclinite was not observed in the bed material of Test G02. Potassium bicarbonate could not exist in the high temperatures of the gasifier due to the fact that it decomposes between 100 and 120°C, and hence was most likely formed by reaction of potassium carbonate (K₂CO₃) with

ambient H₂O and CO₂ after the experiment finished and cooled down, according to the reverse of reaction (1). The sodium analog of reaction (1) is well known in literature due to the use of NaHCO₃ as a fire retardant (eg. [14]).



3.2.4 Mechanism of Agglomeration

Together, these findings suggest that the mechanism for agglomerate formation may involve the reaction of potassium carbonate (K₂CO₃), formed in the char, with silicon from the bed material leading to the formation of molten potassium silicates. A possible reaction to describe this process is:



The sodium analog of reaction (2) has been documented previously [15] to form a liquid sodium silicate melt. Further evidence to support this mechanism will come from examining the cross sections of individual bed particles, and finding if there is a sticky layer surrounding particles consisting of potassium and silicon.

3.2 Stage II Results: Gas Compositions

3.3.1 Experimental Observations

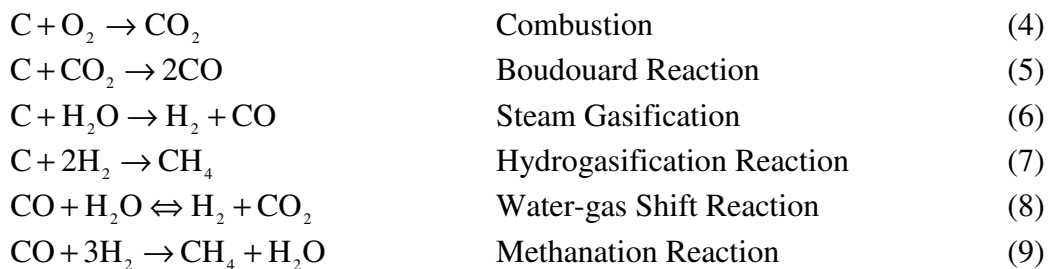
The stage II experiments involved the variation of bed Temperature to determine a range of gas compositions and carbon conversions that are achievable when gasifying Grape Marc. The tests performed were variation of bed temperature for constant air and fuel feed rates. To change the bed temperature, the external heating was adjusted to achieve the desired temperature value.

In each experiment it was assured that the temperature and pressure drop were constant for 30 minutes, indicating the proportion of char and ash was constant for a given run.

3.3.2 Gas Compositions and Carbon conversions

Figure 11 shows the gas composition results. The desired gases of hydrogen and carbon monoxide increased with temperature from approximately 13% and 8%, respectively, at 810°C to 21% and 14%, respectively, at 910°C. Over the same temperature range, carbon dioxide decreased from 16% to 10%. Methane and ethene evolution were approximately constant at 3% and 1% respectively.

In gasification a number of reactions are occurring, summarised by reactions (4)-(9):



The trends with temperature are primarily a function of the reactions (5), (6) and (8). Increasing the bed temperature increases the rate of reactions (5) and (6), implying that more H_2 and CO will form at higher temperatures. This is backed up by Figure 12, based on calculations of carbon conversion for various bed temperatures. As is seen in Figure 12, as the bed temperature increases, the carbon conversion in the gasifier rises from 60 to 85%. This implies that at higher temperatures reactions (5) and (6) are occurring at a much faster rate, and are leading to a higher conversion of char to CO (by reaction with CO_2 and H_2O).

The increase in H_2 is somewhat due to reaction (6), but also the water-gas shift reaction (8). The water gas shift reaction is reversible and the actual gas composition depends on the freeboard temperature and pressure and whether equilibrium is achieved. It is unlikely that equilibrium is achieved in this small reactor owing to the short residence time. Although there was very little moisture present in the fuel (see Table I), reactions with steam can still occur in the gasifier. This is because any hydrocarbons that are burnt in the gasifying air will release steam into the bed, thereby supplying H_2O in reactions (6) and (8).

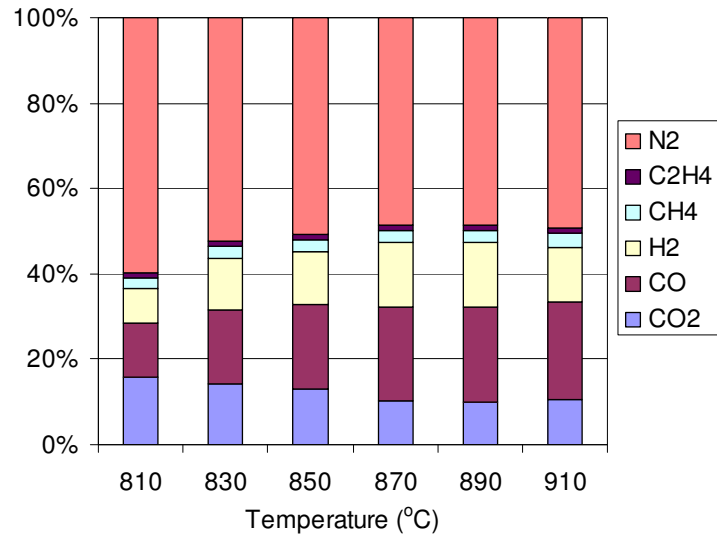


Figure 11 – Bed Temperature effect on Gas composition

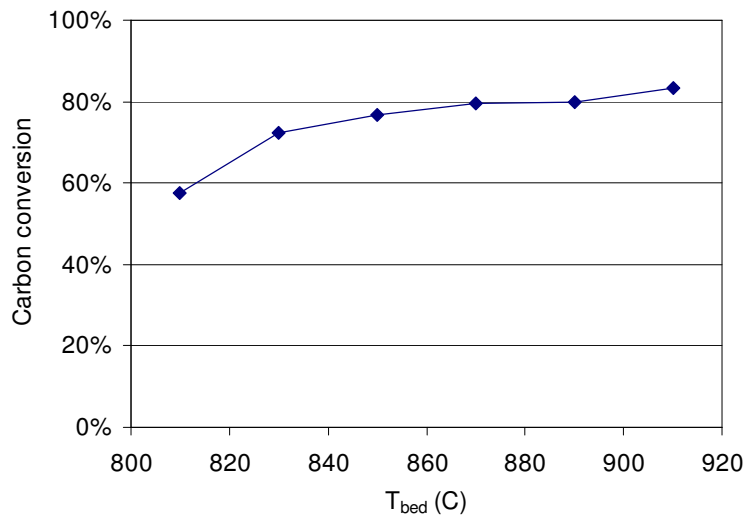


Figure 12 – Carbon conversion versus bed Temperature

3.4 Stage III Results

3.4.1 Stage III observations

The tests in this series were conducted to establish whether gasification of grape stalks causes bed material agglomeration and/or defluidisation. Stage III tests were Tests G11-G15 presented in Table II.

Tests G11-G14 had the following common features:

- (1) Each test had large problems during startup due to temperature instabilities
- (2) Each test led to defluidisation
- (3) The bed at the end of each test was full of agglomerates

Point (1) above was found to be due to feeding problems of the fuel. Compared to grape marc, which has approximately spherical particles, grape stalks are fibrous in nature. This fibrous nature led to intermittent feeding of the fuel particles, which led to temperature disturbances in the bed. At some points the bed temperature rose to levels that could have contributed to agglomeration and defluidisation, as noted in points (2) and (3). It should be noted that occasionally similar temperature fluctuations occurred in the stage I tests, but the rises in temperature did not result in defluidisation, implying that the stalks had a more severe propensity for bed defluidisation and agglomeration than the grape marc.

Test G14 and G15 were gasification of a grape marc / grape stalks mixture. The amount of grape stalks in the mixture was 21%, a value that was determined from industry reported marc/stalks ratios [17]. These tests were to establish whether using a mixture of the two types helped to prevent agglomeration/defluidisation issues. Test G14 suffered from feeding problems and hence had similar results to G11-G13. Conversely, Test G15 was very carefully fed with material to ensure that there were no feeding problems, and hence 100 minutes of trouble free operation was obtained. This result suggests that by careful operation the grape marc and stalks can be gasified together.

Samples of tests G12 and G13 were analysed for ash chemistry to determine the mechanism of agglomerate formation during fluidised bed gasification of grape stalks. SEM was used to examine formation and morphology of bed material agglomerates, morphology of ash coating on the bed sand material and to analyse the chemical composition of these materials.

3.4.2 SEM Analysis

Figure 13 shows an SEM micrograph of a fused agglomerate from test G12, and Figure 14 shows the analysis of the chemical composition for Frames 1-4 in Figure 13. Frames 1-3 show that the chemicals present are fused/glossy in nature, whereas Frame 4 appears to be crystalline. Referring to Figure 14 it is possible to infer that the substance in Frames 1-3 is high in potassium and silicon, with a smaller amount of sodium (3-5%), magnesium (1-5%) and calcium (10-15%). In comparison, Frame 4 is mostly calcium and magnesium.

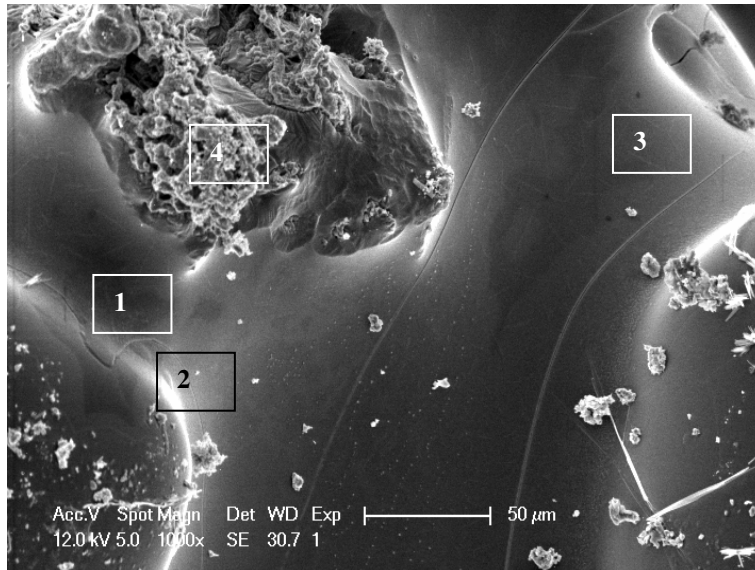


Figure 13 - SEM micrograph of fused agglomerate from Test G12

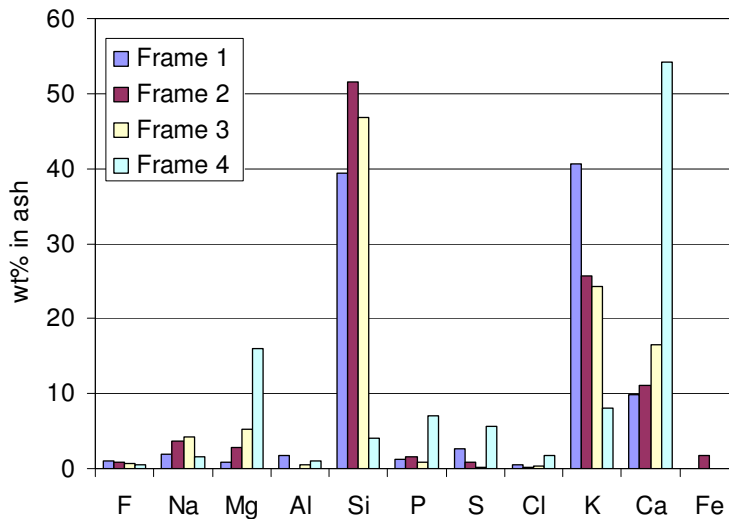


Figure 14 – SEM specific analyses on a carbon and oxygen free basis of Fig 13

Figure 15 shows an SEM micrograph of another agglomerate from test G12, and Figure 16 shows the analysis of the chemical composition for Frames 1-3 in Figure 15. The join between the particles (Frames 1 and 3) show a substantial amount of potassium and silicon, whereas the ash coating on the particle (Frame 2) has a significant amount of calcium, magnesium and phosphorus. Frame 2 also has substantial potassium and silicon. This suggests that the ash coating on the particles has a “glue” of potassium silicates, with inclusions of fly ash in the “glue”.

All the ash contains a small (but important) amount of sodium, implying that the sodium in the original stalks is potentially part of the silicates that are formed. Table VII shows a comparison of the joints in an agglomerate from grape marc gasification versus grape stalks gasification. It is clear that there is 2.2 times as much sodium in the agglomerate joint of grape stalks gasification, compared to grape marc. This would likely add to the formation of sodium-potassium-silicate glasses that cause agglomeration, and may have led to the defluidisation that was observed.

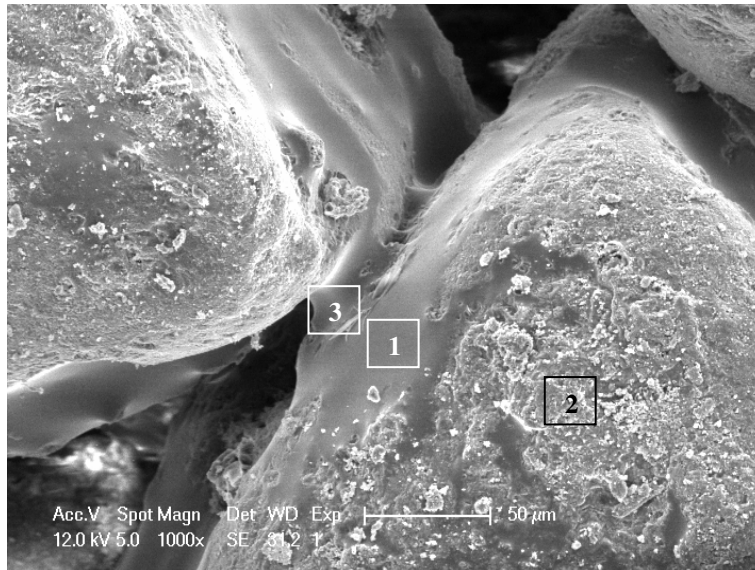


Figure 15 - SEM micrograph of fused agglomerate from Test G12

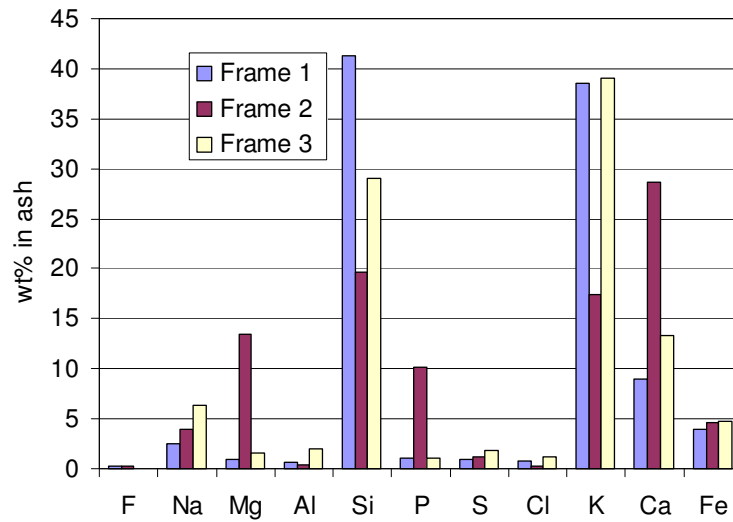


Figure 16 – SEM specific analyses on a carbon and oxygen free basis of Fig 15

Table VII: Comparison between SEM specific analyses on a carbon and oxygen free basis for Marc and Stalks gasification agglomerates

	Marc Agglomerate Joint wt%	Stalks Agglomerate Joint wt%
Na	2.81	6.27
Mg	3.05	1.61
Al	1.88	1.97
Si	36.83	29.06
P	0.00	1.06
S	0.00	1.82
Cl	0.00	1.13
K	52.70	39.00
Ca	2.73	13.32
Fe	0.00	4.75

Figure 17 shows an SEM micrograph of the cross section of an agglomerate from Test G02. An analysis of the chemical composition for the points and frames in Figure 17 are given in Figure 18.

Figure 17 and 18 show that the sticky layer on all of the bed material is consistently high in potassium and silicon. Unlike the grape marc tests, the cross section shows a non-negligible amount of sodium, which originates from the stalk fuel. The calcium and magnesium that are present are due to fly ash within the sticky layer on the particles.

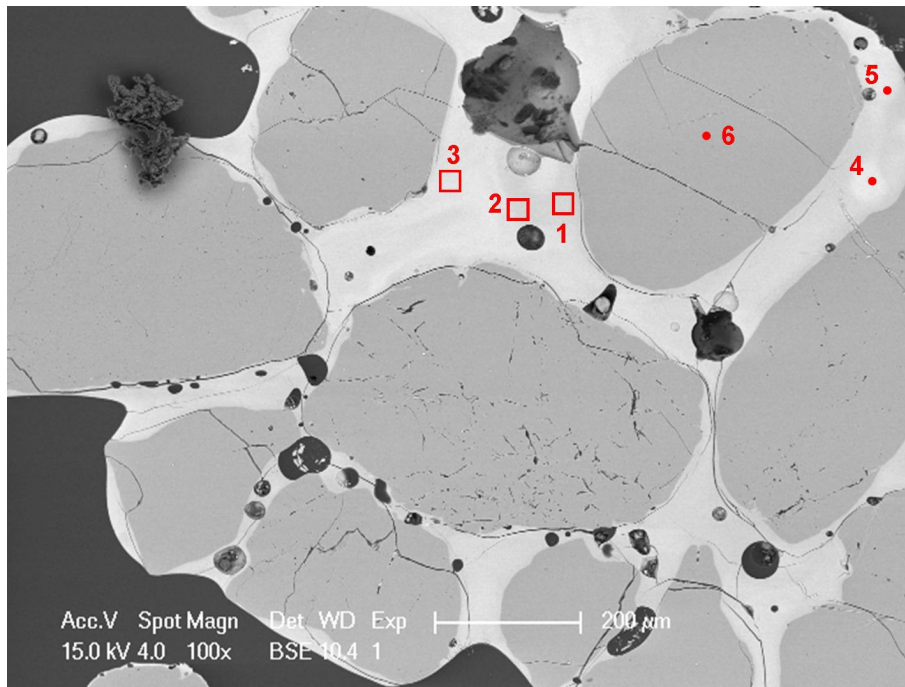


Figure 17 - SEM micrograph of the cross section of an agglomerate from Test G12

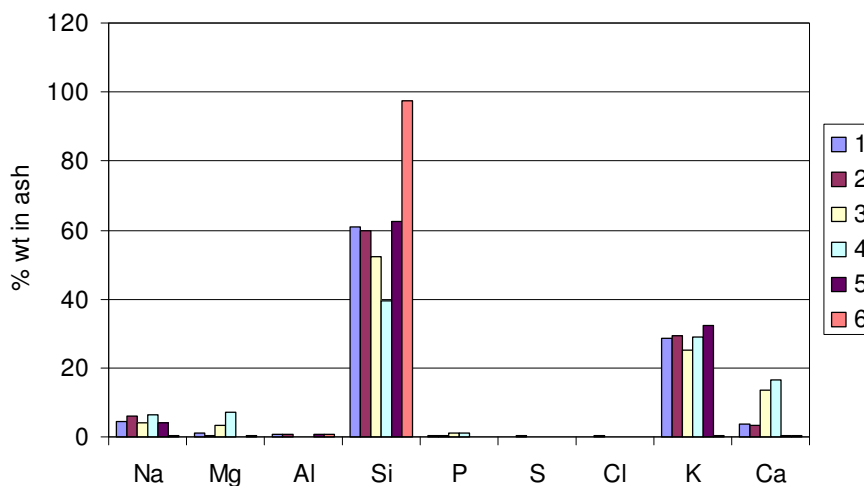


Figure 18 – SEM specific analyses on a carbon and oxygen free basis of Fig 17

Test G13 was gasification of grape stalks in a char bed. The results from this test provide valuable information of the char ash behaviour during gasification. Figure 19 shows an SEM micrograph of a char particle taken from Test G13, and Figure 20 shows the analysis of the chemical composition for Frames 1 and 2 in Figure 19. The important features of Figure 20 are the high potassium and chlorine contents on the surface of the char, and the relatively high sodium content compared to the marc char.

It appears that potassium carbonate, sodium chloride, and potentially potassium chloride are forming in the ash layer on the surface of the char particle. When these char particles make contact with silica grains in the bed material, there is potential for the formation of sodium- and potassium-silicates, which would be fused/glossy at the temperatures of fluidised bed gasification.

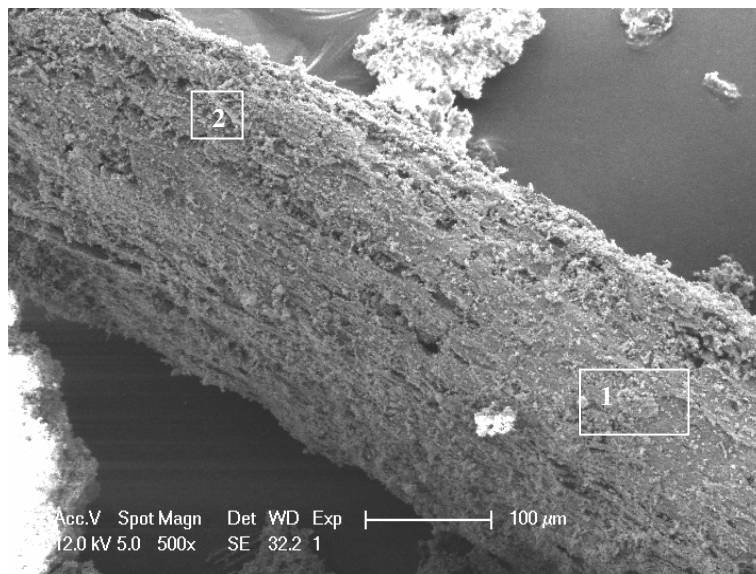


Figure 19 - SEM micrograph of Char particle from Test G13

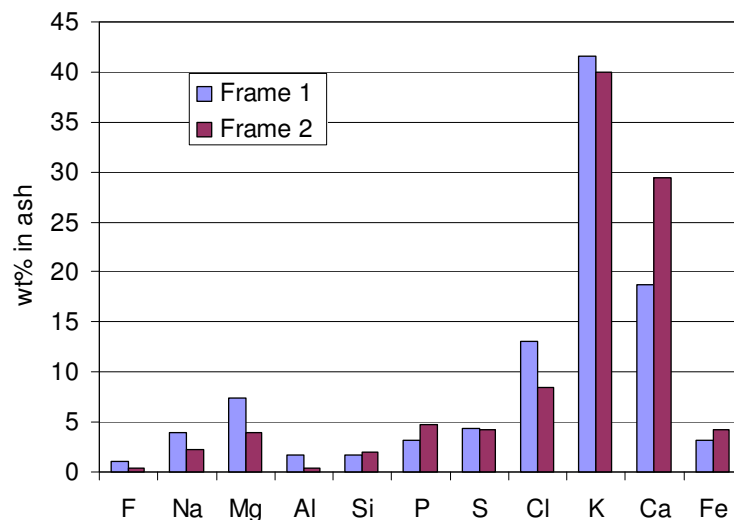


Figure 20 – SEM specific analyses on a carbon and oxygen free basis of Fig 19

Table VIII shows the ash layer composition of grape marc char versus grape stalks char from fluidised bed gasification tests. The major differences are the sodium and chlorine contents. The grape stalk char had ~3 times as much sodium in the ash layer than the grape marc char. The grape marc char had an insignificant amount of chlorine, whereas the stalks char had >10% on a carbon and oxygen free basis. The presence of higher quantities of sodium and chlorine could have led to additional formation of low melting point silicate glasses, as discussed in section 3.4.3 next.

Table VIII: Comparison between SEM specific analyses on a carbon and oxygen free basis for Marc and Stalks gasification

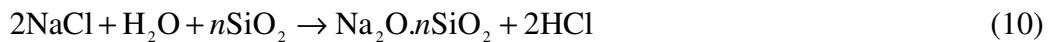
	Grape Marc Char wt%	Grape Stalks Char wt%
Na	1.01	3.15
Mg	3.75	5.65
Al	1.94	1.06
Si	2.69	1.85
P	5.53	4.01
S	3.75	4.29
Cl	0.00	10.71
K	66.04	40.80
Ca	15.30	24.09
Fe	0.00	3.68

3.4.3 Mechanism of Agglomeration

Together, these findings suggest that the mechanism for the bulk formation of agglomerates probably involve the reaction of potassium carbonate (K_2CO_3), formed in the char, with silicon from the bed material leading to the formation of molten potassium silicates. This is described by reaction (2), as discussed in section 3.2.3.



Another route for agglomerate formation during fluidised bed gasification of stalks involves reactions of NaCl or KCl. As described in section 3.4.2, there is a presence of large quantities of chlorine in the char particle during gasification. This would be most likely bound to sodium or potassium in the char. Reactions could hence occur between NaCl or KCl and the silica in the bed material by the reactions (10) and/or (11):



These types of reactions have been reported in literature [18]. Reactions (10) and (11) are considered slower than reactions similar to (2), but nevertheless may be occurring under the conditions of stalk gasification. Further evidence to support this mechanism will come from examining the cross sections of individual bed particles, and determining the chemical nature of the sticky layer surrounding particles.

3.5 Stage IV results

3.5.1 Stage IV observations

The tests in this series were conducted to establish whether fluidised bed combustion of grape marc and/or grape stalks causes bed material agglomeration and/or defluidisation. Stage III tests were Tests C01-C02 presented in Table II.

For test C01, smooth continuous operation was maintained for 200 minutes. Test G02 was only run for 30 minutes due to feeding issues similar to those discussed in section 3.4.1. During the 200 minutes of test C01 and the 30 minutes of test C02, there was a relatively steady temperature in the bed of 860°C. Test C02 had temperature fluctuations after this point, but it was concluded that this was not due to the ash chemistry, but it was actually due to problems with the feeding of biomass to the bed. At the end of each run, agglomerates were found in the bed material and were hence analysed to determine the mechanism of agglomeration.

Samples of tests C01 and C02 were analysed using SEM to examine formation and morphology of bed material agglomerates.

3.5.2 SEM Analysis

Figure 21 shows an SEM micrograph of a fused agglomerate from test C01 – combustion of grape marc. Figure 22 shows the analysis of the chemical composition for Frames 1-3 in Figure 21. It can be seen from Figure 21 that frames 1 and 3 are glossy in appearance, indicating that the nature is non-crystalline. Conversely, frame 2 appears crystalline in nature.

From Figure 22, it appears that Frames 1 and 3 are predominantly potassium and silicon, with frame 3 having a lower silicon content, but higher sulphur content. Frame 2 has a high potassium content, but a much lower silicon content, and a moderate sulphur content. It appears likely that the glossy structure of frames 1 and 3 is due to potassium silicates. There is also a presence of potassium-calcium sulphates in frame 2.

The sulphate formation is a common occurrence in combustion of high alkali high sulphur fuels [7, 8]. The sulphur content of is not very high in grape marc (<0.2%), but under combustion conditions it is likely that most of the sulphur will form sulphates with potassium and calcium. The remaining potassium will form potassium silicates by a similar mechanism to gasification.

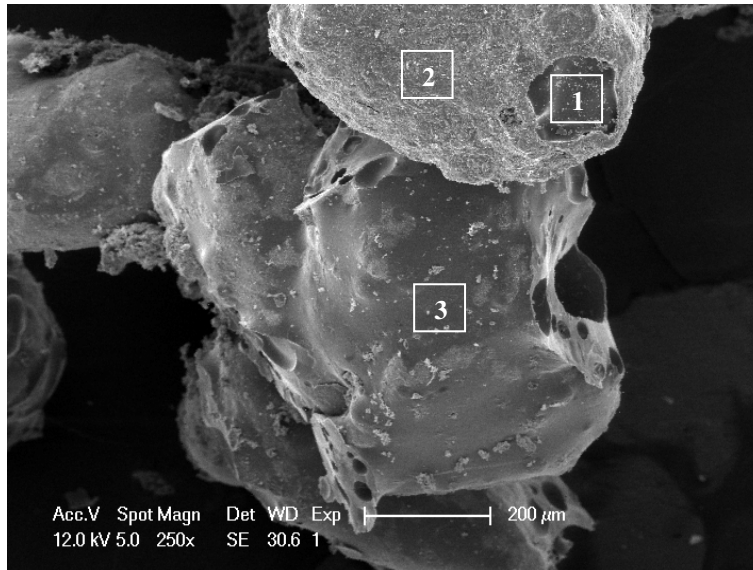


Figure 21 - SEM micrograph of a fused agglomerate from Test C01

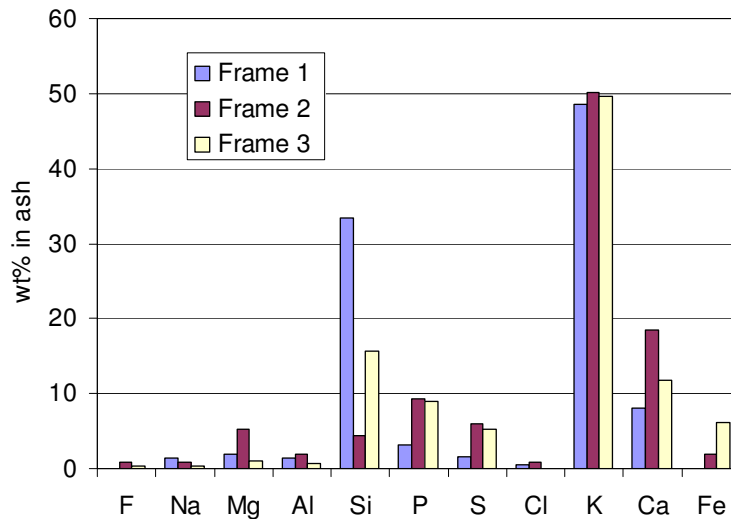


Figure 22 - SEM specific analyses on a carbon and oxygen free basis of Fig 17

Figure 23 shows an SEM micrograph of the cross section of an agglomerate from Test C01. An analysis of the chemical composition for the points and frames in Figure 23 are given in Figure 24.

Figure 23 and 24 show that the sticky layer on all of the bed material is consistently high in potassium and silicon. The calcium and magnesium that are present are due to fly ash within the sticky layer on the particles. Unlike Figure 21 and 22, there is an apparent lack of sulphur which indicates that sulphates are not the cause of the agglomeration, as previously suggested. Instead, it appears that sulphates are deposited on the sticky layer of potassium silicates.

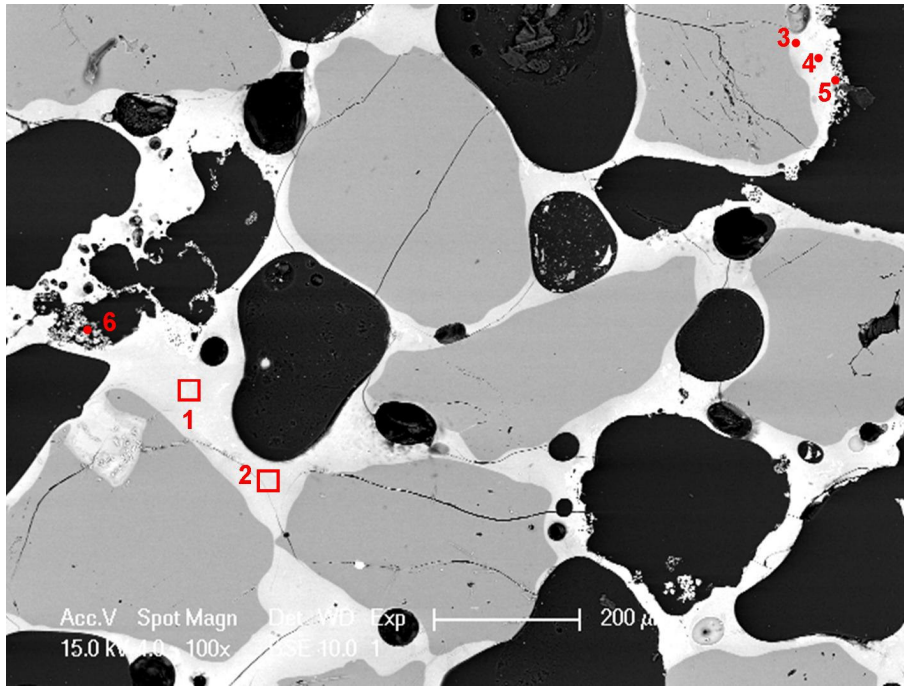


Figure 23 - SEM micrograph of the cross section of an agglomerate from Test C01

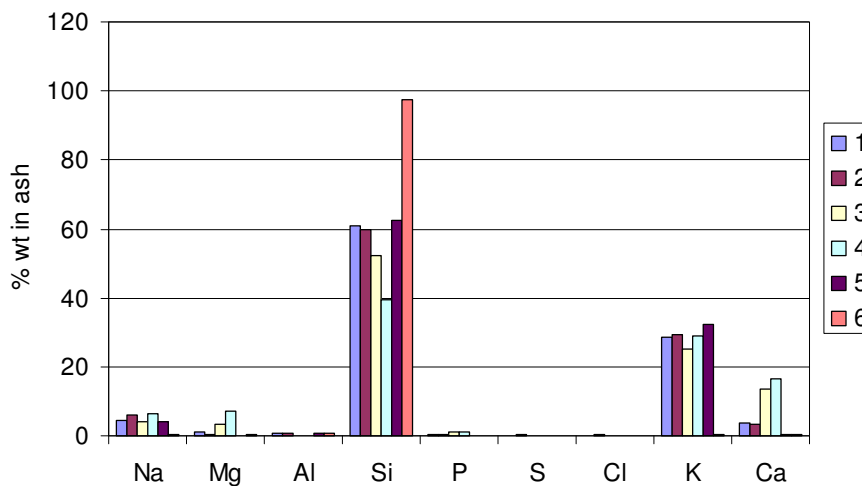


Figure 24 - SEM specific analyses on a carbon and oxygen free basis of Fig 23

Figure 25 shows an SEM micrograph of an agglomerate from test C02 – combustion of grape marc and grape stalks. Figure 26 shows the analysis of the chemical composition for the frame 2 and spots 1 and 3 in Figure 25. It can be seen from Figure 25 that spot 3 are glossy in appearance, indicating that the nature is non-crystalline. Conversely, spot 1 and frame 2 appear crystalline in nature. Figure 26 shows that spot 3 is predominantly potassium and silicon. Spot 1 and Frame 2 have a high potassium content, a high calcium content, but a much lower silicon content, and a moderately high sulphur content. Hence, it appears that spot 1 and frame 2 are mainly potassium calcium sulphates, whereas spot 3 is most likely potassium silicates.

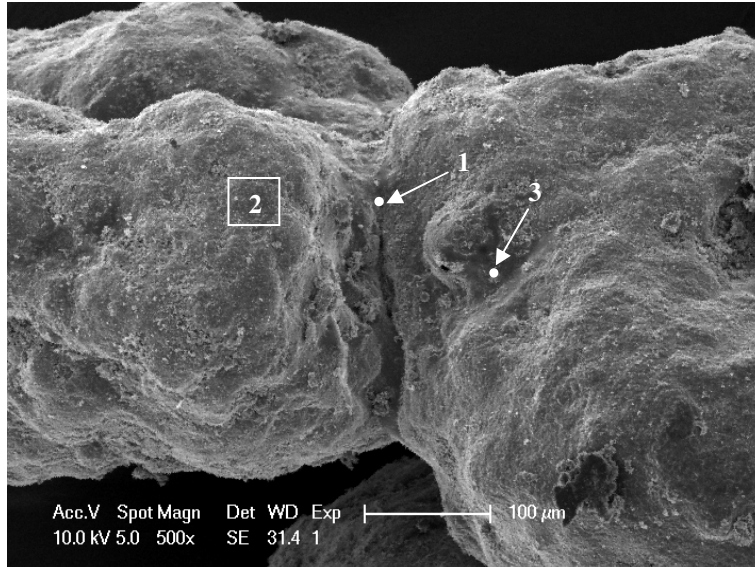


Figure 25 - SEM micrograph of agglomerate from Test C02

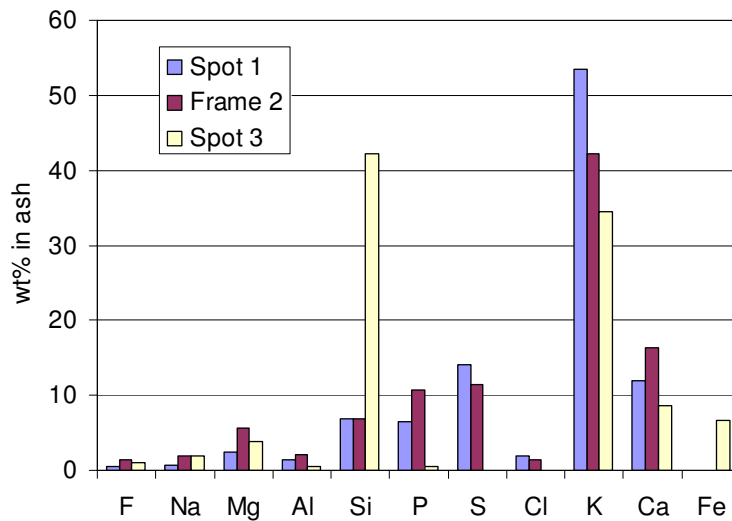


Figure 26 - SEM specific analyses on a carbon and oxygen free basis of Fig 25

Figure 27 shows an SEM micrograph of the cross section of an agglomerate from Test C02. An analysis of the chemical composition for the points and frames in Figure 27 are given in Figure 28.

Figure 27 and 28 show that the sticky layer on all of the bed material is consistently high in potassium and silicon. The calcium, phosphorus and magnesium are present in significant amounts at some points, primarily due to fly ash within the sticky layer on the particles. Frames 1 and 2 show that the true sticky substance that binds the agglomerate together is primarily potassium and silicon.

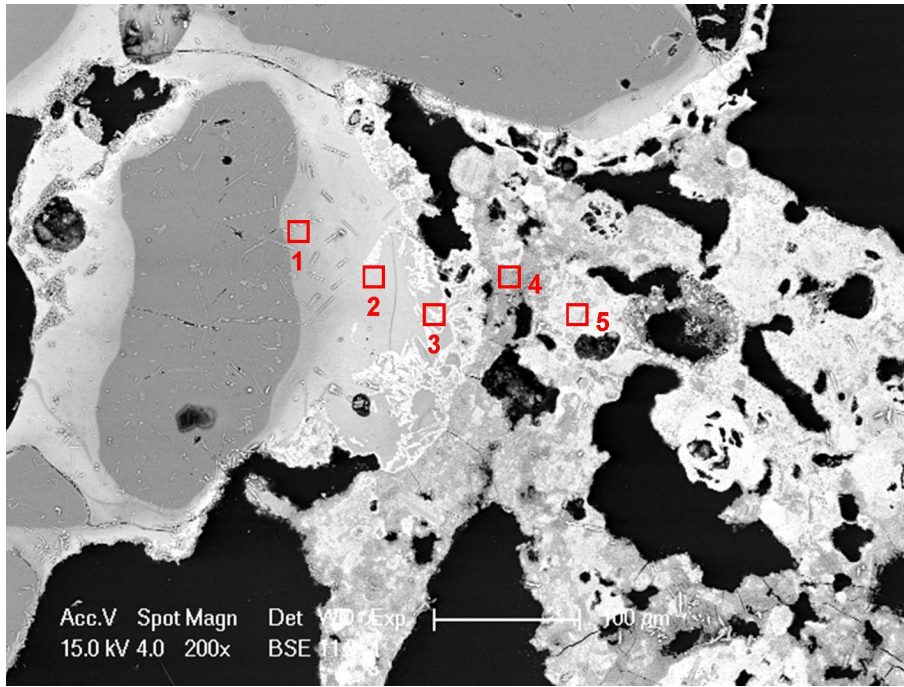


Figure 27 - SEM micrograph of the cross section of an agglomerate from Test C02

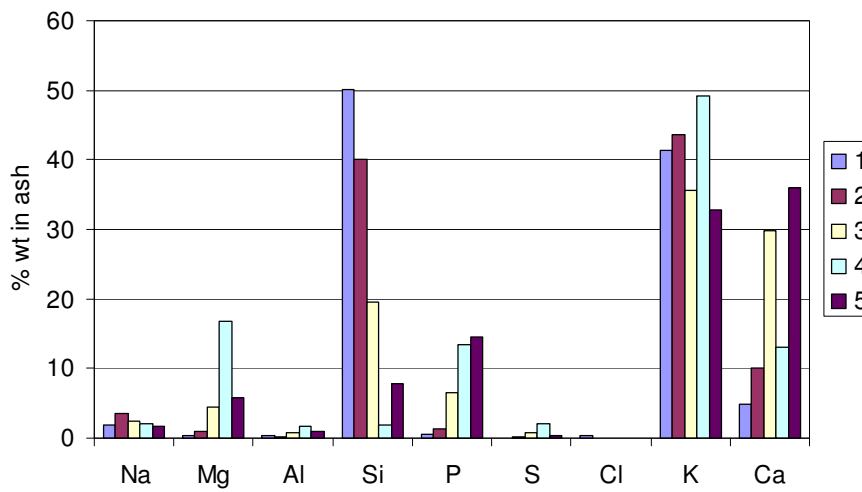


Figure 28 - SEM specific analyses on a carbon and oxygen free basis of Fig 27

3.5.3 Mechanism of Agglomeration

During combustion, a very similar agglomeration mechanism is apparent to that of gasification. It appears that potassium silicates are forming the sticky layer around individual silica particles, thus causing agglomeration. Potassium-calcium sulphates may be forming with the available sulphur in the fuel. There is, however, not enough sulphur in the fuel to form sulphates with the large amount of potassium in the fuel.

4 CONCLUSIONS AND RECCOMENDATIONS

4.1 Conclusions from Stage I

Experiments on the gasification of grape marc in a laboratory scale circulating fluidised bed (CFB) has provided insight into the potential use of grape marc in a fluidised bed gasifier coupled with a gas turbine or gas engine. For all tests, smooth continuous operation was maintained for up to 200 minutes. There was a relatively steady temperature, and the pressure drop over the bed rose only slightly over the period of test in each case due to the build up of ash and unburnt char in the bed.

However, on close examination of the bed material collected after the CFB had cooled down, agglomerates of bed particles were discovered. Scanning Electron Microscopy and X-Ray Diffraction were used to analyse the chemical, morphological and mineralogical nature of the agglomerates. A possible mechanism for agglomerate formation was proposed where potassium carbonate (K_2CO_3) formed in the char reacts with silica from the bed material leading to the formation of molten potassium silicates.

4.2 Conclusions from Stage II

From the Stage II experiments the following conclusions are drawn:

- The higher the bed temperature achievable in a real plant, the better the CO and H₂ concentrations, as well as the conversion of carbon in the original coal. This will probably depend on the limit set by the ash behaviour of the coal.
- Addition of wet fuel into the gasifier will increase the reactions with steam, thereby forming more H₂. Further experiments are needed to examine the gas compositions that are possible with raw grape marc.
- Due to the fact that the hydrogen and carbon contents of the stalks are very similar to the grape marc, similar results are expected for gasification of stalks.

4.3 Conclusions from Stage III

Experiments were undertaken on grape stalks into agglomerate formation during gasification in a laboratory scale CFB. For four out of five tests, serious problems were encountered during the start up period. There were large inconsistencies in the temperature in the bed, mostly brought about by problems in feeding the fibrous stalk particles to the CFB. Regardless, useful information on the formation of agglomerates was collected.

On close examination of the bed material collected after the CFB had cooled down, many agglomerates of bed particles were discovered. Scanning Electron Microscopy was used to analyse the chemical and morphological nature of the agglomerates. A possible mechanism for agglomerate formation was proposed where potassium carbonate (K_2CO_3) formed in the char reacts with silica from the bed material leading to the formation of molten potassium silicates. Another route for formation of silicates from grape marc gasification was proposed whereby the sodium chloride and/or

potassium chloride in the fuel could react to also form potassium and/or sodium silicates.

4.3 Conclusions from Stage IV

Experiments were undertaken on grape marc and a mixture of grape marc and stalks into agglomerate formation during combustion in a laboratory scale CFB. For the grape marc tests, smooth continuous operation was maintained for up to 200 minutes. There was a relatively steady bed temperature, and the pressure drop over the bed rose only slightly over the period of the test in each case due to the build up of ash in the bed. For the mixture of grape marc and stalks, serious problems were encountered during the start up period. There were large inconsistencies in the temperature in the bed, mostly brought about by problems in feeding the fibrous stalk particles to the CFB. Regardless, useful information on the formation of agglomerates was collected.

On close examination of the bed material collected after the CFB had cooled down, agglomerates of bed particles were discovered. Scanning Electron Microscopy was used to analyse the chemical and morphological nature of the agglomerates. An agglomeration mechanism was proposed where potassium silicates form in the bed, leading to sticky layers on the bed particles.

4.5 Recommendations

Mineralogical analysis by XRD will provide information on any crystal structure compounds that are present. This will hence help in understanding the agglomeration behaviour of stalks CFB gasification and marc and stalks CFB combustion.

Further research to develop and verify mitigation strategies for agglomerate formation is required in order to utilize grape marc and/or stalks for gasification or combustion at a large scale.

6 REFERENCES

1. Winemakers Federation of Australia (2009), 2009 WFA Vintage Report, <http://www.wineaustralia.com/australia/LinkClick.aspx?fileticket=RxY7bRwtxz0%3d&tabid=5419>
2. Muhlack, R. (2008) “Filling the potholes in the environmental research landscape” Proceedings – Australian Society of Viticulture and Oenology Seminar – Footprints, food miles and furphies, 10 Sept 2008
3. P. McKendry, *Bioresource Technol* 83(1) (2002) 47–54.
4. Australian Government Department of Agriculture, Fisheries and Forestry (2006), Wine Industry Factsheet, http://www.daff.gov.au/__data/assets/pdf_file/0006/183183/wine_industry_factsheet_september_2006.pdf
5. Australian Government Department of Foreign Affairs and Trade (2008), Agriculture and the WTO, http://www.dfat.gov.au/trade/negotiations/trade_in_agriculture.html
6. M. Bartels, W. Lin, J. Nijenhuis, F. Kapteijn, J. R. van Ommen, *Prog. Energy Combust. Sci.* 34 (2008) 633–666.
7. A. R. Manzoori, and P. K. Agarwal, *Fuel* 71 (1992) 513-522.
8. H. B. Vuthaluru, D. –K. Zhang, T. M. Linjewile, *Fuel Process Technol.* 67 (2000) 165-176.
9. M. R. Dawson, and R. C. Brown, *Fuel* 71(1992) 585-592.
10. B.-J. Skrifvars, G. Sfiris, R. Backman, K. Widegren-Dafgård, and M. Hupa, *Energy Fuels* 11 (1997) 843-848.
11. L. H. Nuutinen, M. S. Tiainen, M. E. Virtanen, S. H. Enestam, and R. S. Laitinen, *Energy Fuels* 18 (2004) 127-139.
12. E. Brus, M. Ohman, and A. Nordin, *Energy Fuels* 19 (2005) 825-832.
13. R. A. Durie (Ed.), *The Science of Victorian Brown Coal: Structure, Properties and Consequences for Utilization*, Butterworth Heinmann, Oxford, UK (1991), pp. 270.
14. D. Bakirtzis, M.A. Delichatsios, S. Liodakis, and W. Ahmed, *Thermochimica Acta* 486 (2009) 11–19.
15. P. Hrma, *J. American Ceramic Society* 68 (6) (1985) 337-341.
16. K.O. Davidsson, L.-E. Åmand, B.-M. Steenari, A.-L. Elled, D. Eskilsson, B. Leckner, *Chemical Engineering Science* 63 (2008) 5314-5329.
17. R. Muhlack, Private Communication, Based on Estimate from Constellation Wines, 2006.
18. W.D. Halstead and E. Raask, *Fuel* 42 (1969), pp. 344–349.

APPENDIX A: TGA Results for Winery Waste Biomass

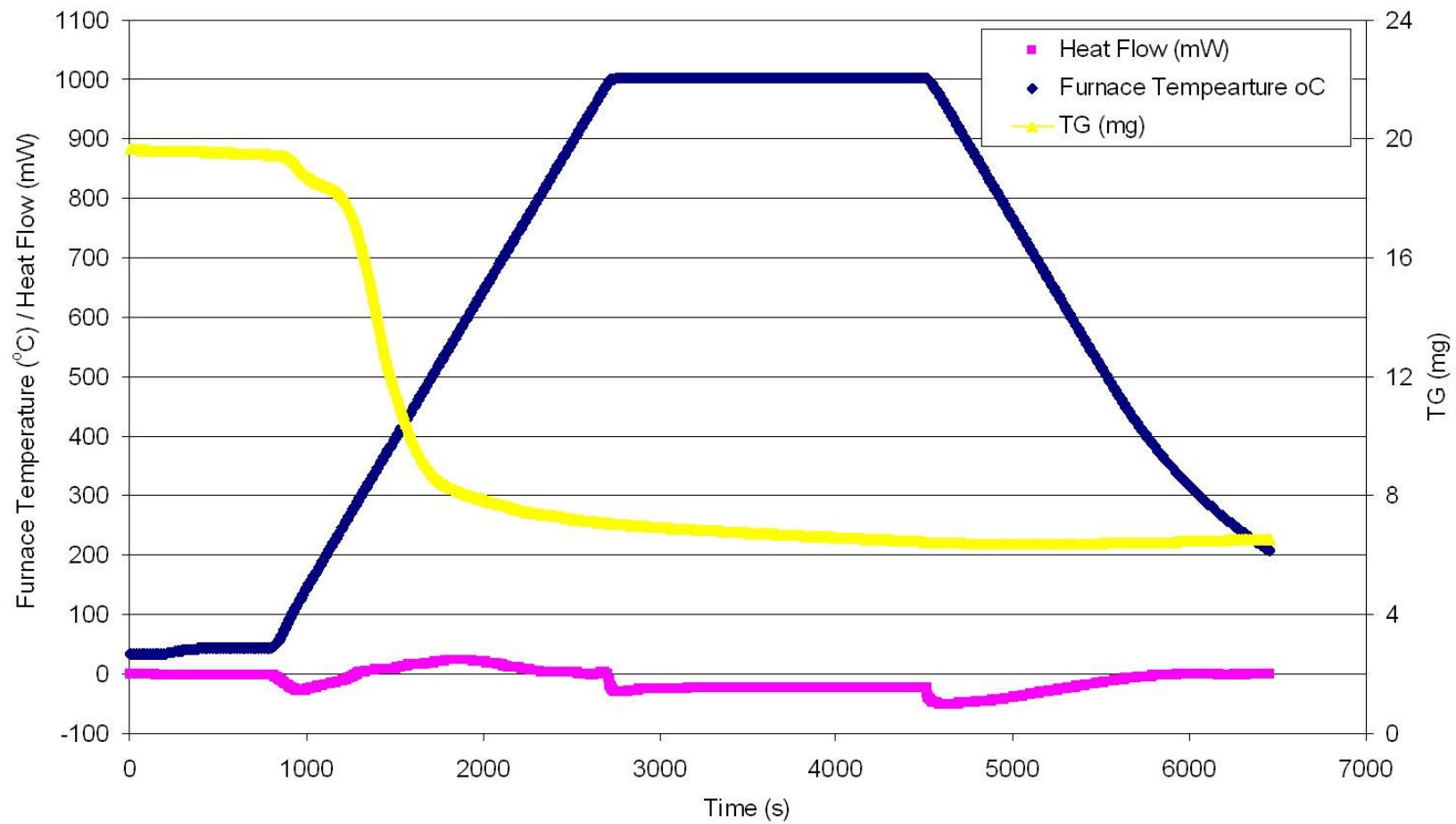


Figure A1 – TGA Results for Grape Marc in N₂ at 30°C/min

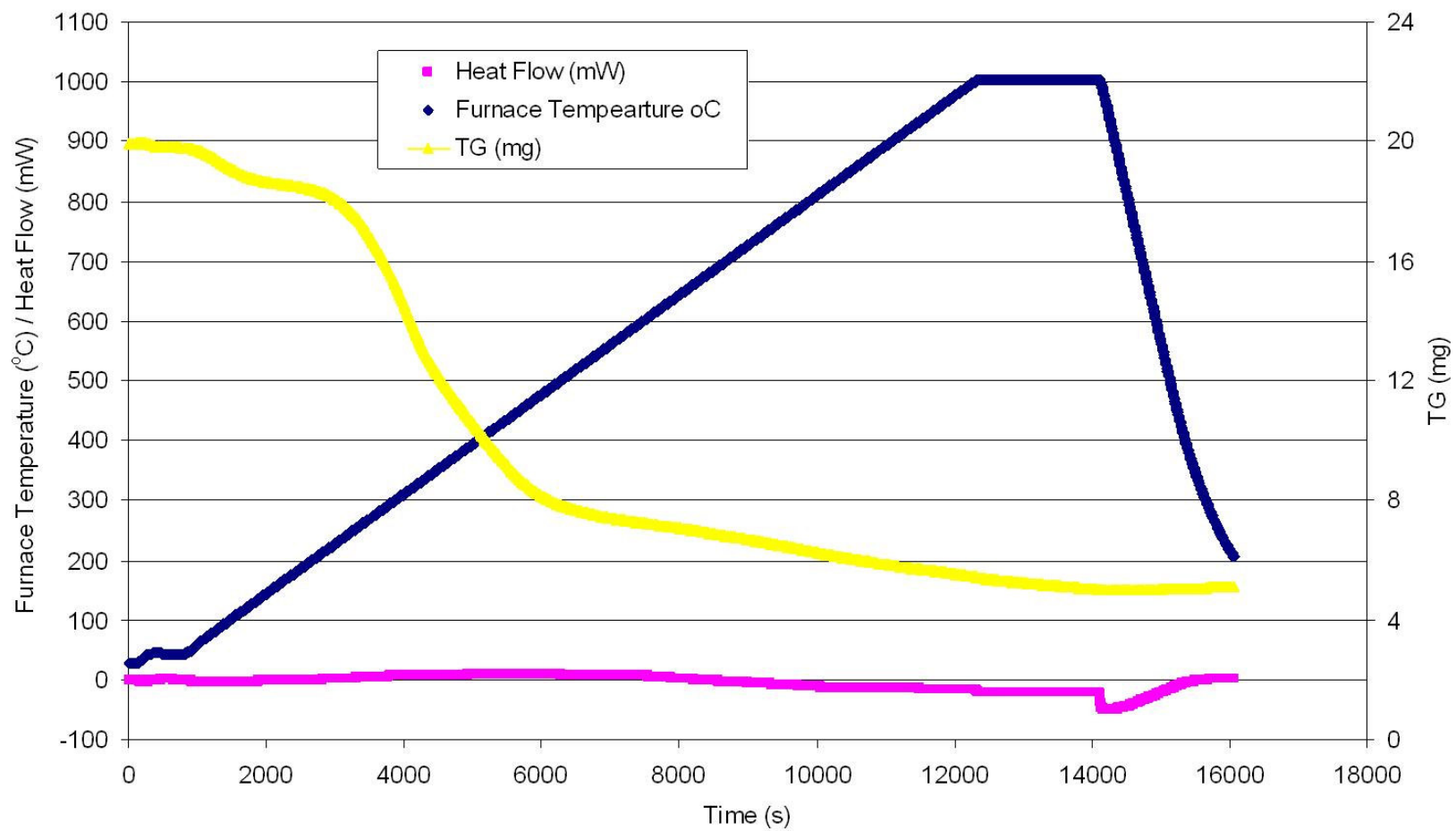


Figure A2 – TGA Results for Grape Marc in N₂ at 5°C/min

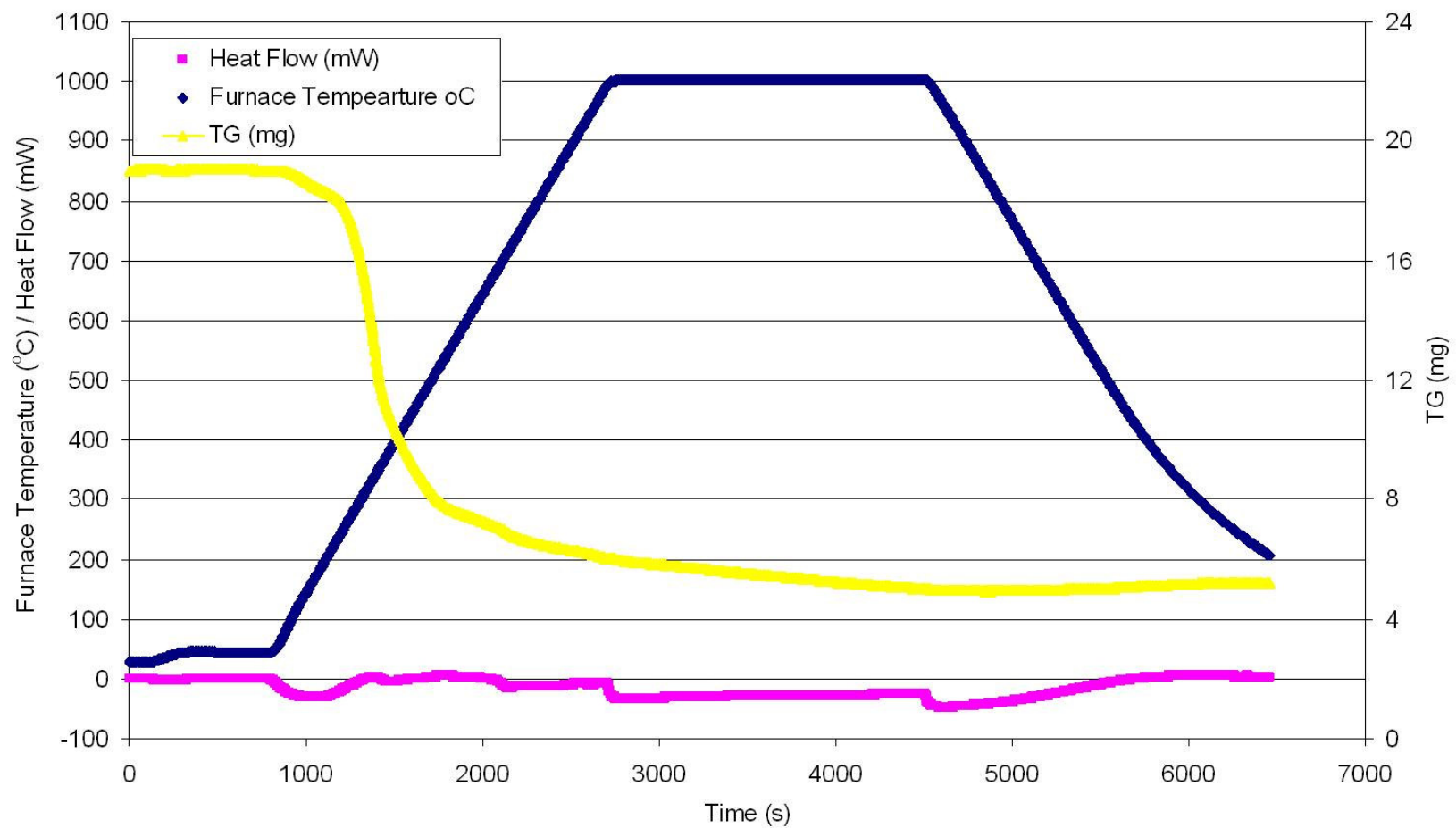


Figure A3 – TGA Results for Grape Stalks in N₂ at 30°C/min

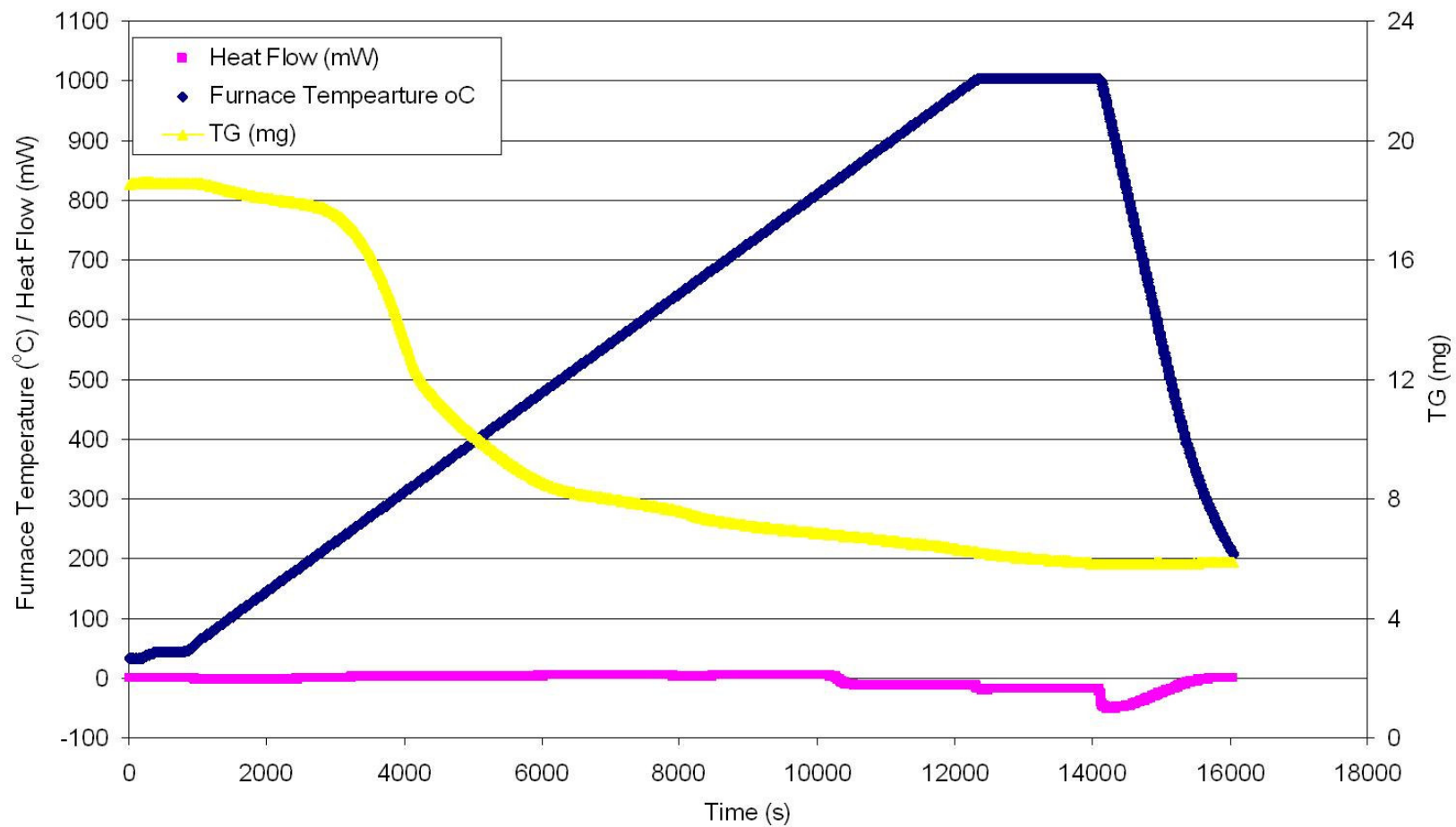


Figure A4 – TGA Results for Grape Stalks in N₂ at 5°C/min

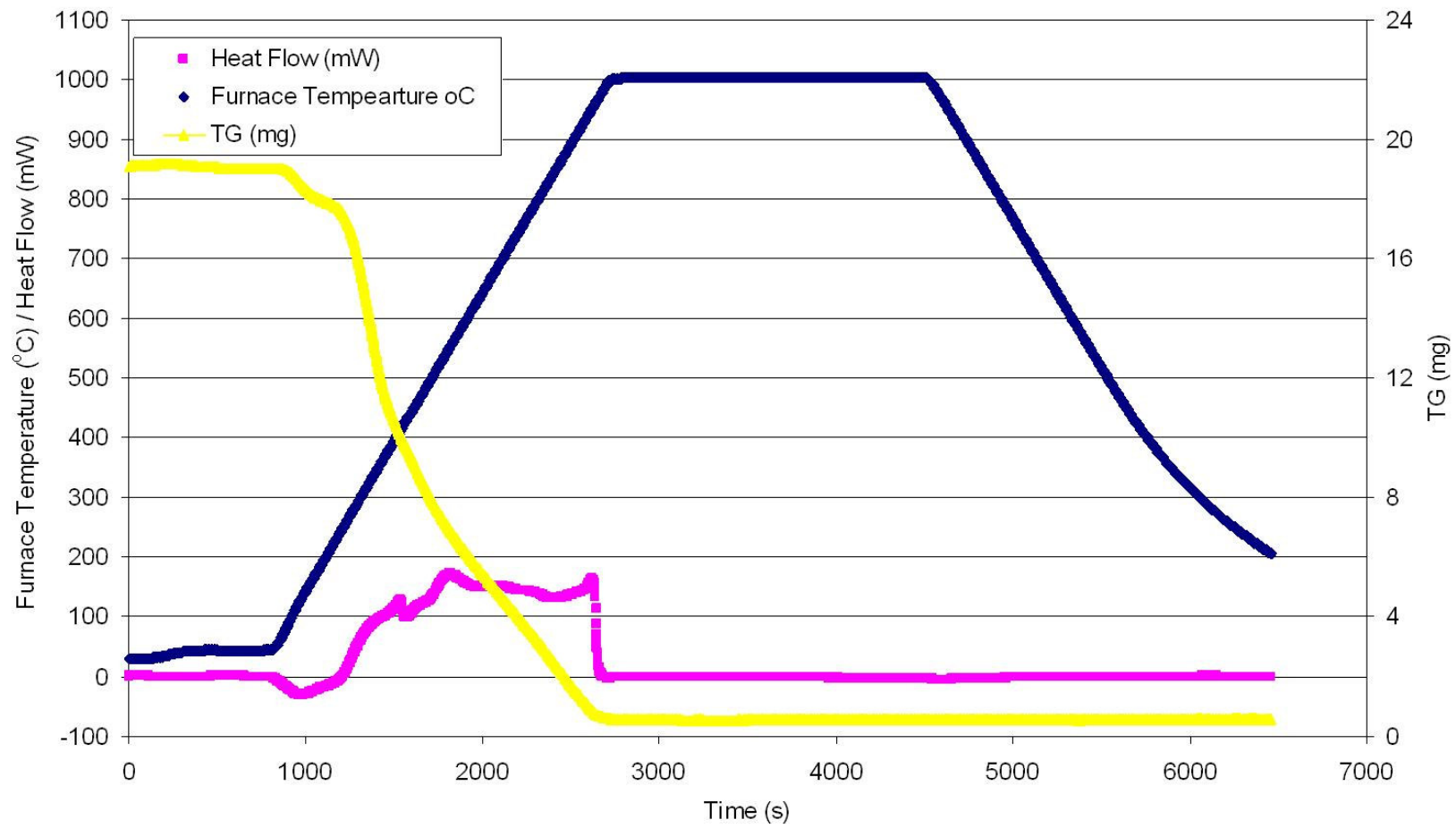


Figure A5 – TGA Results for Grape Marc in Air at 30°C/min

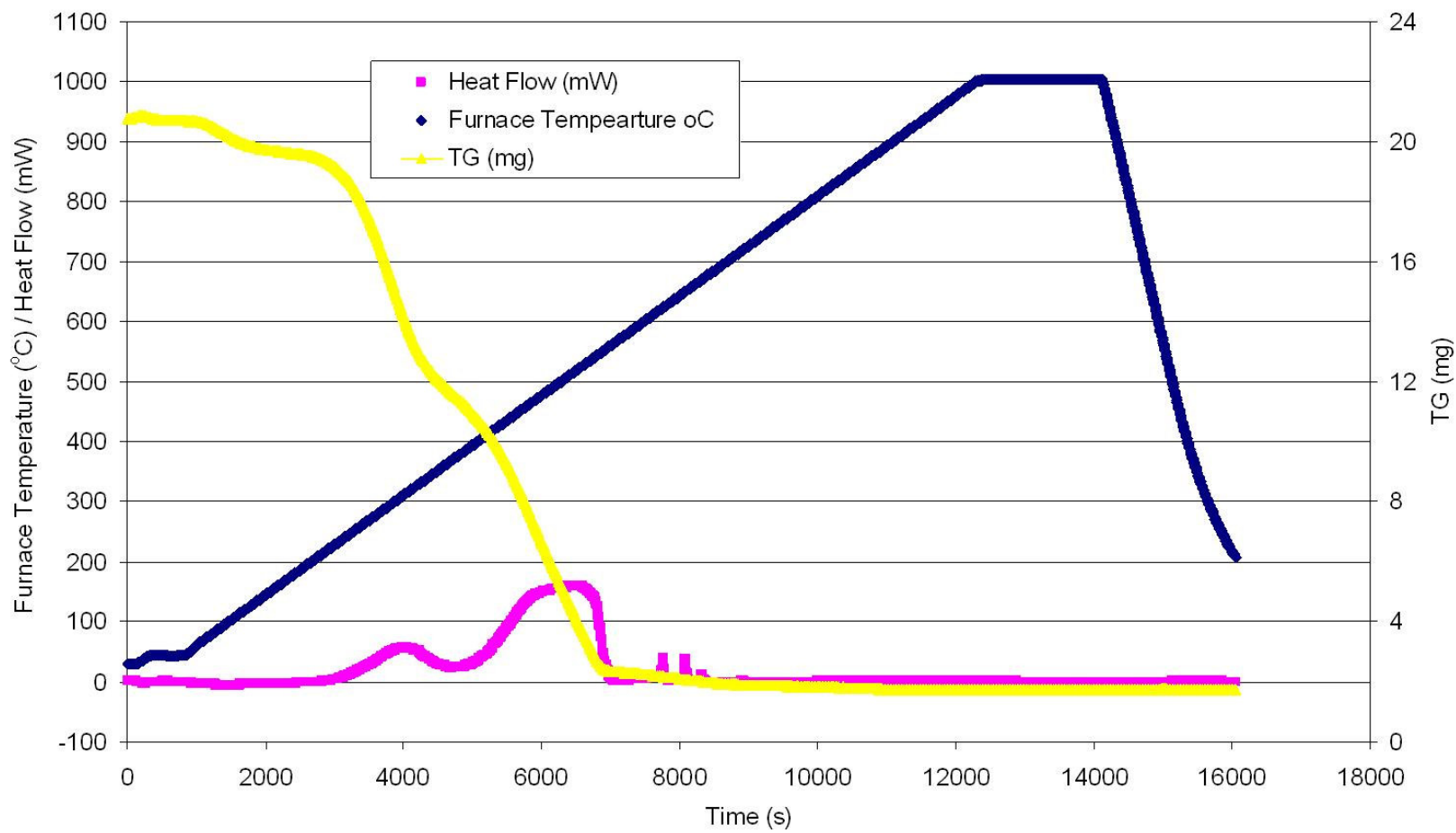


Figure A6 – TGA Results for Grape Marc in Air at 5°C/min

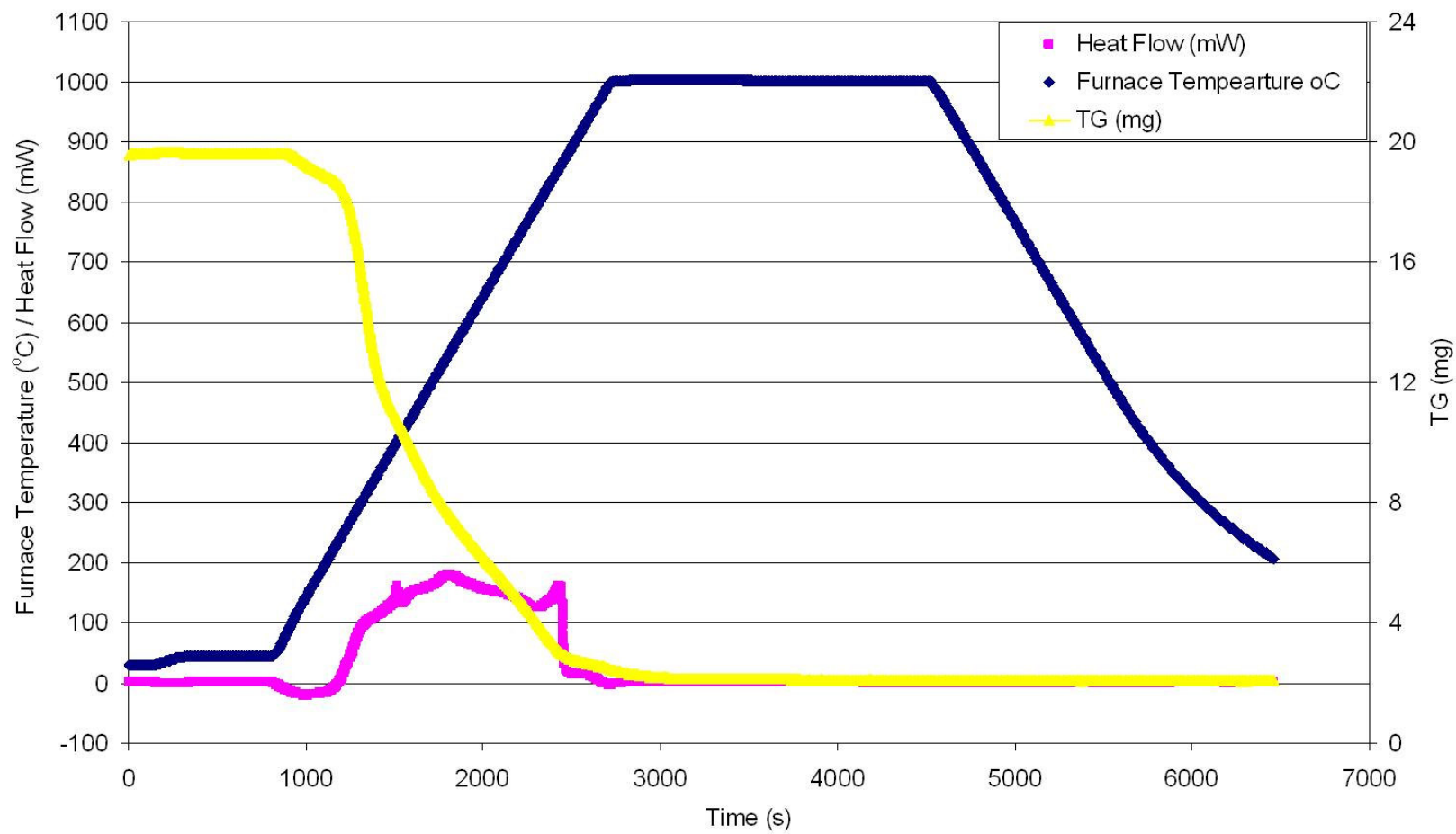


Figure A7 – TGA Results for Grape Stalks in Air at 30°C/min

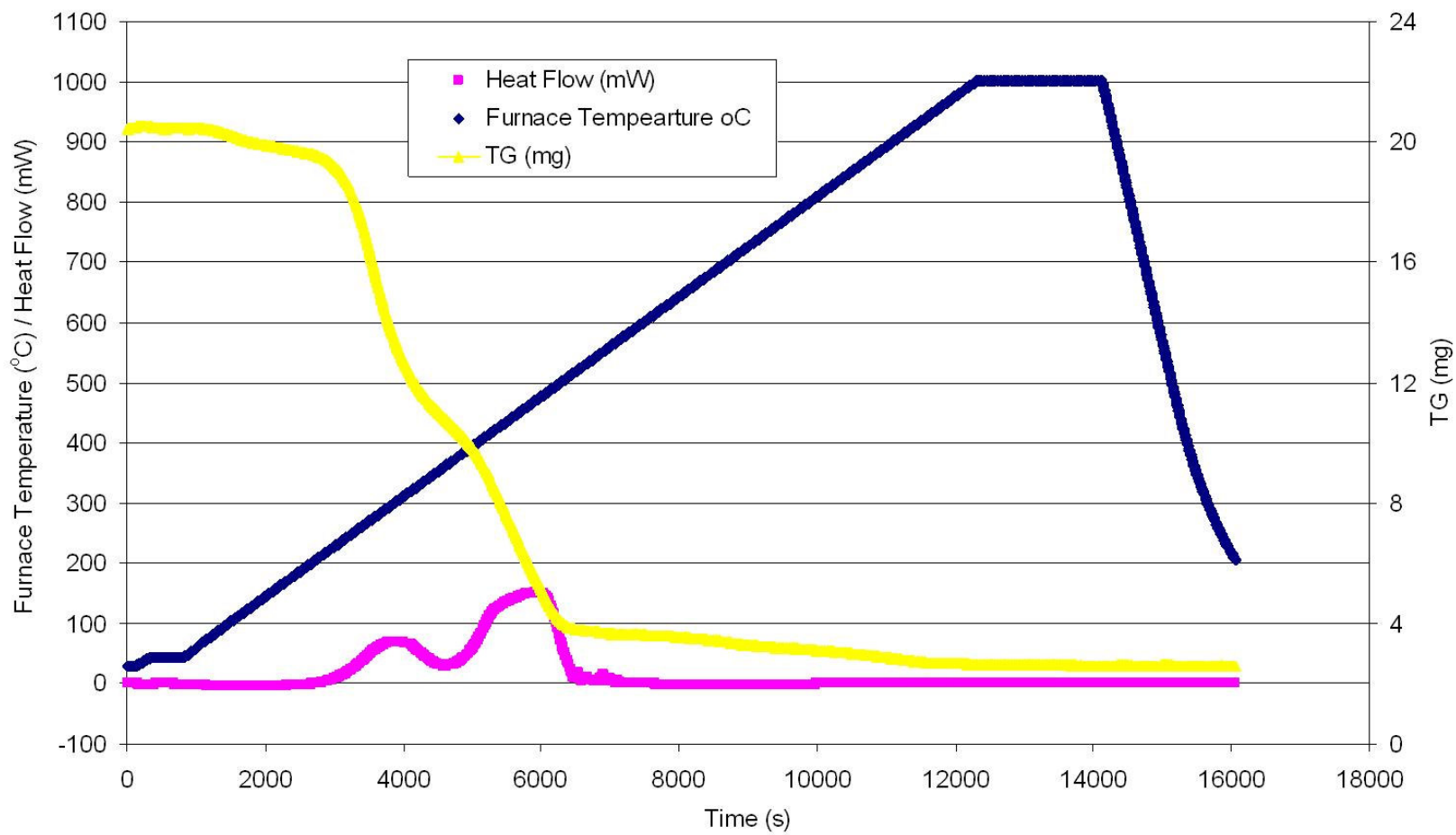


Figure A8 – TGA Results for Grape Stalks in Air at 5°C/min